Neutron Matter with Skyrme Functionals in a Periodic External Field

by

Samuel Martinello

A Thesis

Presented to

The University of Guelph

In partial fulfilment of requirements

for the degree of

Master of Science

in

Physics

Guelph, Ontario, Canada

ABSTRACT

NEUTRON MATTER WITH SKYRME FUNCTIONALS IN A PERIODIC EXTERNAL FIELD

Samuel Martinello
University of Guelph, 2020

Advisor:
Professor Alexandros Gezerlis

As a basis for the understanding of both the structure of neutron stars as well as their dynamics in neutron star mergers and their contributions to nucleosynthesis, we provide insight into the composition of neutron matter in a neutron star's crust. We discuss the Skyrme-Hartree-Fock model for infinite neutron matter in the presence of a periodic external field. We study the Skyrme effective interaction and discuss its benefits as well as its limitations in providing an effective model. We are able to compute the energies, densities, wavefunctions as well as the linear density-density response functions for infinite neutron matter across a wide range of initial system configurations. Finally, we are able to establish these methods as an effective yet simple model for studying large nuclear systems.

Acknowledgements

There are an incredible number of people through their guidance and help that I owe this research.

First and foremost, I would like to thank my advisor Alexandros Gezerlis. His expertise as well as his patience while helping me maneuver through the academic process proved invaluable, and I am a better person for having been able to work under his guidance. I would also like to thank my advisory and defence committees: Liliana Caballero, Dennis Muecher, and Elisabeth Nicol.

My colleagues Matt Buracyznski, Nawar Ismail, George Palkanoglou, Will Dawkins, Bernie Ross, Anish Verma and Tash Zielinski as well as the nuclear physics group all helped provide important perspectives on my research as well as friendship and camaraderie throughout my tenure.

Finally, I would like to thank my parents: my mother Patricia and my father Ron, for supporting me in every way possible for these past years.

I extend special thanks to Compute Canada and SHARCNET for providing computational resources.

Contents

List of Tables

List of Figures

Chapter 1

Introduction

The examination of neutron matter properties provides an important basis for the understanding of the structure and dynamics of neutron stars. Most often, the composition of neutron stars is described hydrodynamically as a nuclear fluid through the equation of state (EoS). The common approach to constructing an EoS is to begin with a thermodynamically motivated potential, considering only the intensive system variables in thermodynamic equilibrium [1]. Many such EoS profiles are motivated by the observation of X-ray bursts, neutron star oscillations, and gravitational radiation emitted by both pulsars and through neutron star mergers [2]. These observations can then be fit to a host of EoSs motivated by general relativity, with the most standard being those derived from the Tolman-Oppenheimer-Volkoff eqations [3, 4, 5, 6]. Alternatively, the EoS may be be built through nuclear many-body methods; where both ab initio and phenomenological approaches are frequently used. These include, but are not limited to: Brueckner-Hartree-Fock methods, Monte Carlo methods, Skyrme-type forces and mean-field theories [7]. Often, these methods are parameterized through nuclear energy density functionals of many forms [8, 9, 10].

As an extension of these problems, energy density functional theories may be

used to probe more specifically the structure of neutron star crusts. These are often modeled as an infinite neutron matter sea with a periodic network of nuclei interspersed. These nuclei provide a periodic potential external to the neutron sea and give rise to a host of scenarios often studied through the lens of nuclear response theory [11, 12, 13, 14, 15, 16].

1.1 Nuclear Hamiltonian

For the purpose of this research, we will model the interactions in neutron matter by a Skyrme-type interaction. Skyrme's interaction approximates the nuclear potential through the composition of two- and three-body effective interaction terms $v_{ij}^{(2)}$ and $v_{ijk}^{(3)}$. Since this potential aims to have the ability to describe a many-body system, the $v_{ij}^{(2)}$ terms will approximate the two-body interaction of nucleons whereas the three-body term $v_{ijk}^{(3)}$ encapsulates all of the higher order many-body effects. In general, it is possible to continue to introduce higher order terms to describe the many-body interactions, however, the potential is truncated at the three-body term to aid in the ease of calculation:

$$V = \sum_{i<j} v_{ij}^{(2)} + \sum_{i<j<k} v_{ijk}^{(3)} \tag{1.1}$$

The two-body interaction may be written as a short range expansion in configuration space of the form [17, 18]:

$$\begin{aligned} v_{ij}^{(2)} &= t_0(1 + x_0 P_\sigma)\delta(\mathbf{r}_1 - \mathbf{r}_2) + \tfrac{1}{2}t_1(1 + x_1 P_\sigma)[\delta(\mathbf{r}_1 - \mathbf{r}_2)\mathbf{P}^2 + \mathbf{P}'^2\delta(\mathbf{r}_1 - \mathbf{r}_2)] \\ &\quad + t_2(1 + x_2 P_\sigma)\mathbf{P}' \cdot \delta(\mathbf{r}_1 - \mathbf{r}_2)\mathbf{P} + iW_0(\sigma_1 + \sigma_2) \cdot \mathbf{P}' \times \delta(\mathbf{r}_1 - \mathbf{r}_2)\mathbf{P} \end{aligned} \tag{1.2}$$

Where P_σ is a spin-exchange operator and the $\sigma_{1,2}$ are the Pauli spin matrices. The $t_s, x_s : s = 1, 2, 3$ parameterize the mean central potential and W_0 parameterizes the

spin-orbit coupling. All are free parameters corresponding to the constraints of the system. Additionally, the $\mathbf{P}$ is the operator $(\nabla_1 - \nabla_2)/2i$ acting to the right and $\mathbf{P}'$ is the operator $-(\nabla_1 - \nabla_2)/2i$ acting to the left. The three-body interaction potential is similarly a zero range interaction of the form:

$$v_{ijk}^{(3)} = t_3\delta(\mathbf{r}_1 - \mathbf{r}_2)\delta(\mathbf{r}_2 - \mathbf{r}_3) = \frac{1}{6}t_3(1 + x_3P_\sigma)\delta(\mathbf{r}_1 - \mathbf{r}_2)\rho\Big(\frac{\mathbf{r}_1 + \mathbf{r}_2}{2}\Big)^\alpha \tag{1.3}$$

parameterized by the density ρ and the parameters t_3, x_3 and σ. It is important to notice that both the two-body and three-body interactions are each written in terms of δ-distributions. The benefits of this form are twofold: it provides a simple integrable form as well as accurately approximating a Gaussian central potential with exchange terms of the form:

$$V = e^{-|\mathbf{r}_1 - \mathbf{r}_2|/\mu}(W + BP_\sigma - HP_\tau - MP_\sigma P_\tau) \tag{1.4}$$

with range μ, and parameterized by the coefficients W, B, H and M to first order [19]. At this point we now consider a system of N neutrons whose ground state is described by the Slater determinant of the single neutron wavefunctions $\phi_i(x_j) : i = 1, \ldots, N$:

$$\phi(x_1, \ldots, x_N) = \tfrac{1}{\sqrt{N!}}\det|\phi_i(x_j)| \tag{1.5}$$

We note that x_j denotes the tuple $(\mathbf{r}, \sigma)$ of spatial coordinates and spin for a given state. In general, the total energy of the system is given by the expectation value:

$$\begin{aligned} E &= \langle\phi(x_1, \ldots, x_N)|\,(T + V)\,|\phi(x_1, \ldots, x_N)\rangle \\ &= \sum_i \langle i|\,\tfrac{p^2}{2m}\,|i\rangle + \tfrac{1}{2}\sum_{ij}\langle ij|\,\bar{v}_{12}^{(2)}\,|ij\rangle + \tfrac{1}{6}\sum_{ijk}\langle ijk|\,\bar{v}_{123}^{(3)}\,|ijk\rangle \\ &= \int \mathcal{H}_0(\mathbf{r})d^3r \end{aligned} \tag{1.6}$$

where m is the neutron mass and $\bar{v}^{(2)}_{1,2}$, and $\bar{v}^{(3)}_{1,2,3}$ are the antisymmetrizations of the matrix elements $v^{(2)}_{1,2}$ and $v^{(3)}_{1,2,3}$.

Computing the expectation values in Eq. (1.6) we recover the energy density functional $\mathcal{H}_0(\mathbf{r})$ for neutron matter, and it is given by the expression:

$$\mathcal{H}_0 = \mathcal{K} + \mathcal{H}_0 + \mathcal{H}_3 + \mathcal{H}_{\text{eff}} + \mathcal{H}_{\text{fin}} + \mathcal{H}_{so} + \mathcal{H}_{sg} + \mathcal{H}_{Coul} \tag{1.7}$$

Each of these terms represent a different component of the nuclear interaction

$$\begin{aligned}
\mathcal{K} &= \frac{\hbar^2}{2m}\tau(\mathbf{r}) && \text{kinetic energy} \\
\mathcal{H}_0 &= \frac{1}{4}t_0(1-x_0)\rho^2(\mathbf{r}) && \text{zero range} \\
\mathcal{H}_3 &= \frac{1}{24}t_3(1-x_3)\rho^{2+\alpha}(\mathbf{r}) && \text{three body} \\
\mathcal{H}_{\text{eff}} &= \frac{1}{8}\big[t_1(1-x_1)+3t_2(1+x_2)\big]\rho(\mathbf{r})\tau(\mathbf{r}) && \text{effective mass} \\
\mathcal{H}_{\text{fin}} &= \frac{3}{32}\big[t_1(1-x_1)-t_2(2+x_2)\big]\big(\nabla\rho(\mathbf{r})\big)^2 && \text{finite range} \\
\mathcal{H}_{so} &= W_0\mathbf{J}(\mathbf{r})\cdot\nabla\rho(\mathbf{r}) && \text{spin orbit} \\
\mathcal{H}_{sg} &= \big[t_1(1-x_1)-t_2(1+x_2)\big]\mathbf{J}^2(\mathbf{r}) && \text{spin gradient tensor}
\end{aligned}$$

We do not consider the Coulomb interaction component, $\mathcal{H}_{Coul}$, as neutrons are electrically neutral particles. The parameterization we will be considering are the SLy4 infinite neutron matter parameters [20]:

$$t_0 = -2488.91 \text{ MeV fm}^3 \quad , \quad t_1 = 486.82 \text{ MeV fm}^5$$

$$t_2 = -546.39 \text{ MeV fm}^5 \quad , \quad t_3 = 13777.0 \text{ MeV fm}^{3+3\alpha}$$

$$x_0 = 0.834 \quad , \quad x_1 = -0.344 \quad , \quad x_2 = -1.000 \quad , \quad x_3 = 1.254$$

$$\alpha = 1/6 \quad , \quad W_0 = 123.0 \tag{1.8}$$

We note that the definitions of the the neutron density $\rho(\mathbf{r})$, kinetic density $\tau(\mathbf{r})$ and spin density $\mathbf{J}(\mathbf{r})$ follow from the definition of the Slater determinant wavefunction and are expressed in terms of the single particle wavefunctions $\phi_i(\mathbf{r}, \sigma)$:

$$\rho(\mathbf{r}) = \sum_{i,\sigma} |\phi_i(\mathbf{r}, \sigma)|^2 \tag{1.9}$$

$$\tau(\mathbf{r}) = \sum_{i,\sigma} |\nabla\phi_i(\mathbf{r}, \sigma)|^2 \tag{1.10}$$

$$\mathbf{J}(\mathbf{r}) = (-i) \sum_{i,\sigma,\sigma'} \phi_i^*(\mathbf{r}, \sigma)[\nabla\phi_i(\mathbf{r}, \sigma) \times \langle\sigma| \boldsymbol{\sigma} |\sigma'\rangle] \tag{1.11}$$

Finally, we would like to extend the relevance of this energy density functional to beyond infinite homogeneous neutron matter. The crusts of neutron stars are primarily composed of neutron matter with nuclei periodically interspersed throughout. The presence of these nuclei gives rise to a periodic external field. Since we are fundamentally concerned with the response of the neutron matter due to varying periodicities of this field, we choose to examine a cosinusoidal potential for simplicity. This additional term will take the form:

$$v(\mathbf{r}) = 2v_q \cos(\mathbf{q} \cdot \mathbf{r}) \tag{1.12}$$

Where $\mathbf{q}$ is the the wavevector for this field. Without loss of generality, since our infinite neutron matter system is both homogeneous and isotropic by design, we may choose a set of Cartesian axes as our coordinate system such that $\mathbf{q}$ is collinear with the z-axis. As we will later see, this choice of coordinates will greatly simplify the solution process by decoupling each of the axial wavefunction contributions. Thus,

the complete energy density functional may be written as:

$$\mathcal{H}(\mathbf{r}) = \mathcal{H}_0(\mathbf{r}) + v(\mathbf{r})\rho(\mathbf{r}) \tag{1.13}$$

To begin to solve this problem, we will first consider cases of non-interacting neutrons with and without the presence of the external potential $v(\mathbf{r})$; that is, the free Fermi gas and the Mathieu Fermi gas. We will then make use of Hartree-Fock theory to build a full solution to the interacting neutron matter problem. This method makes use of the approximation of the many body wavefunction as a Slater determinant of the individual wavefunctions as outlined in Eq. (1.5) that satisfies antisymmetry properties required for Fermionic systems. We are able minimize the total energy with respect to variations in the single particle wavefunctions through the method of Langrange multipliers:

$$\frac{\delta}{\delta\phi_i}\Big(E - \sum_j e_j \int d\mathbf{r}|\phi_j(\mathbf{r})|^2\Big) = 0 \tag{1.14}$$

From this minimization, we then produce the single particle Hartree-Fock equations:

$$-\nabla\cdot\left(\frac{\hbar^2}{2m^*(\mathbf{r})}\nabla\phi_j(\mathbf{r})\right) + U(\mathbf{r})\phi_j(\mathbf{r}) + v(\mathbf{r})\phi_j(\mathbf{r}) = e_j\phi_j(\mathbf{r}) \tag{1.15}$$

which will later be derived in Chapter 3.

Chapter 2

Fermi Gas

2.1 Non-interacting Free Fermi Gas

As a preliminary step to building the full-fledged solution to the interacting neutron matter problem, we must first characterize the properties of an infinite system of a free, non-interacting Fermi gas (FFG) in three dimensions. In free space, the single particle spatial wavefunctions $\phi_i(\mathbf{r})$ are governed by the basic free particle Hamiltonian:

$$\hat{H} = -\frac{\hbar^2}{2m}\nabla^2 \tag{2.1}$$

where the time independent Schrödinger equation is given by the partial differential equation:

$$-\frac{\hbar^2}{2m}\nabla^2\phi_i(\mathbf{r}) = e_i\phi_i(\mathbf{r}) \tag{2.2}$$

where e_i is the associated eigenenergy to the state $\phi_i(\mathbf{r})$. At this point we must now recognize that while the infinite free particle problem does provide a complete solution set that may be found analytically, when moving to the interacting Fermi gas problem

this property will be lost. Additionally, although the solution set is complete, it is non-normalizable. As such, important properties of the system, such as the density, cannot be extracted. To combat this problem, we consider the solutions for a finite subset of N particles contained in a periodic box of volume $V = L^3$, where the infinite system will be modeled by an infinite tessellation of these periodic boxes. This is done under the assumption that for large enough N, the subset will provide an accurate approximation to the infinite system and the observed properties of the subset will be equivalent to the properties of the infinite system in the thermodynamic limit (TL): $N \to \infty$, $V \to \infty : N/V = \rho$, where ρ is the constant density of the system. This is mathematically expressed by applying the following periodic boundary condition to the single particle wavefunctions:

$$\phi_i(x, y, z) = \phi_i(x + n_1 L, y + n_2 L, z + n_3 L) \quad : \quad n_1, n_2, n_3 \in \mathbb{Z} \tag{2.3}$$

A separation of variables technique using $\phi_i(\mathbf{r}) = \phi_{i,x}(x)\phi_{i,y}(y)\phi_{i,z}(z)$ may be used to decompose Eq. (2.2) into three independent ordinary differential equations:

$$-\frac{\hbar^2}{2m}\frac{d^2}{ds^2}\phi_{i,s}(s) = e_{i,s}\phi_{i,s}(s) \quad : \quad s = x, y, z \tag{2.4}$$

with solutions:

$$\phi_{i,s}(s) = \frac{1}{\sqrt{L}}e^{ik_s s} \quad , \quad e_{i,s}(k_s) = \frac{\hbar^2}{2m}k_s^2 \quad : \quad k_s = \frac{2\pi}{L}n_s \quad , \quad n_s \in \mathbb{Z} \quad : \quad s = x, y, z \tag{2.5}$$

Combining these results, our single particle wavefunction solutions and corresponding

eigenengergies now take the form:

$$\phi_i(\mathbf{r}) = \frac{1}{\sqrt{V}} e^{i\mathbf{k}\cdot\mathbf{r}} \quad , \quad e_i(\mathbf{k}) = \frac{\hbar^2}{2m}\mathbf{k}^2 \quad : \quad \mathbf{k} = \frac{2\pi}{L}(n_x, n_y, n_z) \quad , \quad n_x, n_y, n_z \in \mathbb{Z} \tag{2.6}$$

For a Fermi gas, the lowest energy states are filled first according to the Pauli exclusion principle. In the case of neutrons, a spin-1/2 system, each state may be populated by each of the +1/2 and -1/2 spin projections. With this in place, calculating the energy per particle of the finite system may be simply calculated as the sum of the single particle energies:

$$E_{FFG}(N) = \frac{\hbar^2}{2m} \sum_{|\mathbf{k}|<k_F} \mathbf{k}^2 \tag{2.7}$$

Where $k_F = (2\pi^2\rho)^{1/3}$ is the Fermi wavenumber of the system. This Fermi wavenumber is related to the energy per particle through the Fermi energy in the TL through the expression:

$$E_{FFG}(\infty) = \frac{3}{5}E_F = \frac{3\hbar^2 k_F^2}{10m} \tag{2.8}$$

It is now important to note that since we are only considering a finite subset of particles, finite size (FS) effects will present themselves. As such, an appropriate choice of particle number must be made to mitigate the presence of these FS effects. In Fig. (2.1) we observe characteristic minima in magnitudes of the FS effects at the particle numbers N = 2, 14, 38, 54, 66, ... corresponding to the FFG shell closures. These shell closures occur when all degenerate states below the Fermi energy are fully populated. For calculations done using Monte Carlo methods, a particle number of 66 is often used as it corresponds to a shell closure with relatively small FS effects. Additionally, calculations at higher shell closures are prohibitively expensive

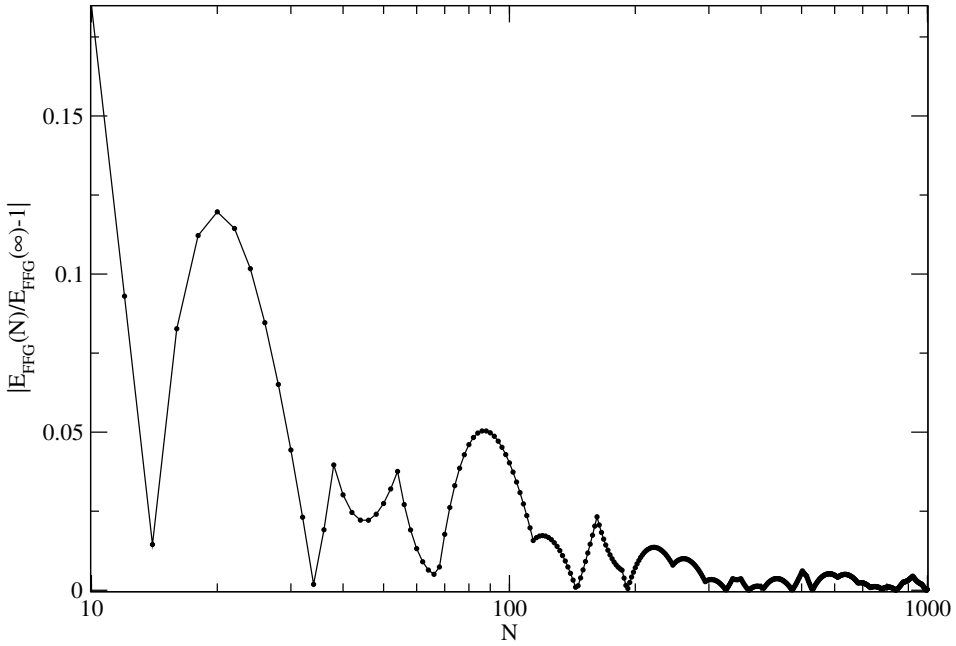

Figure 2.1: Relative error of N particle energy compared to TL energies shows magnitude of finite size effects at a density of $\rho = 0.10$ fm^{-3}.

computationally. However, for the purposes of this work the Hartree-Fock methods that will be used do not have these limitations. To maintain a correspondence with the Monte Carlo simulations we will be using boxes of linear dimensions that are integer multiples of the dimensions of the box containing 66 particles. We found that the box with linear dimensions 4 times that of the box containing 66 particles provided the the most accurate results when compared to boxes of linear dimensions 2 and 3 times that of box containing 66 particles. Additionally, using boxes with linear dimensions of integer order higher than 4 times that of box containing 66 particles did not produce more accurate solutions as the baseline error due to the solution methods used is reached before this point. Thus, we will be studying the case of

$N = 4^3(66) = 4224$ particles.

2.2 Non-interacting Mathieu Fermi Gas

The next logical step we take in building the interacting neutron matter problem is to introduce a periodic external potential. This potential will take the form:

$$v(q, \mathbf{r}) = 2v_q \cos(qz) \quad : \quad q = \frac{2\pi n}{L} \quad , \quad n \in \mathbb{Z} \tag{2.9}$$

where $2v_q$ is the amplitude of the potential, and q is the wavenumber chosen such that an integer number of wavelengths fit into a box of length L. Thus, the single particle FFG Schrödinger equation Eq. (2.2) will be modified to take the form:

$$-\frac{\hbar^2}{2m}\nabla^2\phi_i(\mathbf{r}) + 2v_q \cos(qz)\phi_i(\mathbf{r}) = e_i\phi_i(\mathbf{r}) \tag{2.10}$$

As before, a separation of variables technique using $\phi_i(\mathbf{r}) = \phi_{i,x}(x)\phi_{i,y}(y)\phi_{i,z}(z)$ will be used and we will again recover the one-dimensional FFG Hamiltonian Eq. (2.4) and solutions Eq. (2.5) along the x and y axes. Along the z-axis, the Schrödinger equation reduces to:

$$-\frac{\hbar^2}{2m}\frac{d^2}{dz^2}\phi_{i,z}(z) + 2v_q \cos(qz)\phi_{i,z}(z) = e_{i,z}\phi_{i,z}(z) \tag{2.11}$$

Where $e_{i,z} = e_i - e_{i,x} - e_{i,y}$ since the particles are non-interacting. We make the change of variable $\tilde{z} = qz/2$ so this equation will take a more usable form, thus:

$$\begin{aligned}
&-\frac{\hbar^2 q^2}{8m}\frac{d^2}{d\tilde{z}^2}\phi_{i,\tilde{z}}(\tilde{z}) + 2v_q \cos(2\tilde{z})\phi_{i,\tilde{z}}(\tilde{z}) = e_{i,\tilde{z}}\phi_{i,\tilde{z}}(\tilde{z}) \\
&\frac{d^2}{d\tilde{z}^2}\phi_{i,\tilde{z}}(\tilde{z}) + \left(\frac{8me_{i,\tilde{z}}}{\hbar^2 q^2} - 2\frac{8mv_q}{\hbar^2 q^2}\cos(2\tilde{z})\right)\phi_{i,\tilde{z}}(\tilde{z}) = 0 \\
&\frac{d^2}{d\tilde{z}^2}\phi_{i,\tilde{z}}(\tilde{z}) + \Big(a - 2Q\cos(2\tilde{z})\Big)\phi_{i,\tilde{z}}(\tilde{z}) = 0
\end{aligned} \tag{2.12}$$

This is known as Mathieu's equation, with eigenvalue $a = 8me_{i,\tilde{z}}/\hbar^2 q^2$ and potential amplitude $Q = 8mv_q/\hbar^2 q^2$. We recall that we are only concerned with solutions that obey the periodic boundary condition $\phi_{i,z}(z) = \phi_{i,z}(z + nL) : n \in \mathbb{Z}$ or equivalently $\phi_{i,\tilde{z}}((L/\pi)\tilde{z}) = \phi_{i,\tilde{z}}((L/\pi)\tilde{z} + nL) = \phi_{i,\tilde{z}}((L/\pi)(\tilde{z} + n\pi)) : n \in \mathbb{Z}$. Solutions to Eq. (2.12) of this form belong to a class of solutions known as Floquet solutions. In the most general case, these Floquet solutions may be written as [21]:

$$\phi_{i,\tilde{z}}(\tilde{z}) = Af_1(\tilde{z}) + Bf_2(\tilde{z}) \quad : \quad A, B \in \mathbb{C} \tag{2.13}$$

where there always exists a solution in terms of a characteristic exponent ν and a π-periodic function $p(\tilde{z})$ of the form:

$$f_1(\tilde{z}) = e^{i\nu\tilde{z}}p(\tilde{z}) \quad : \quad \nu \in \mathbb{C} \tag{2.14}$$

Both $p(\tilde{z})$ and $f_2(\tilde{z})$ will be determined by the choice of ν. Due to the nature of our problem, the requirement that $\phi_{i,\tilde{z}}(\tilde{z})$ is both bounded and 2π-periodic imposes the condition that ν must take on only integer values. The function $f_2(\tilde{z})$ then takes the form:

$$f_2(\tilde{z}) = C\tilde{z}f_1(\tilde{z}) + f_3(\tilde{z}) \quad : \quad C \in \mathbb{C} \quad , \quad f_3 : \mathbb{R} \to \mathbb{C} \tag{2.15}$$

where $f_3(\tilde{z})$ has the same periodicity as $f_1(\tilde{z})$. However, this function will be discarded as it is unbounded. With these conditions in place, the eigenvalues and eigenfunctions of Eq. (2.12) may be deduced. These solutions are the Mathieu cosine functions and eigenvalues:

$$ce_n(\tilde{z}, Q) \quad , \quad a_n(Q) \quad : \quad n = 0, 1, 2, \ldots \tag{2.16}$$

and the Mathieu sine functions and eigenvalues:

$$se_n(\tilde{z}, Q) \quad , \quad b_n(Q) \quad : \quad n = 1, 2, 3, \ldots \tag{2.17}$$

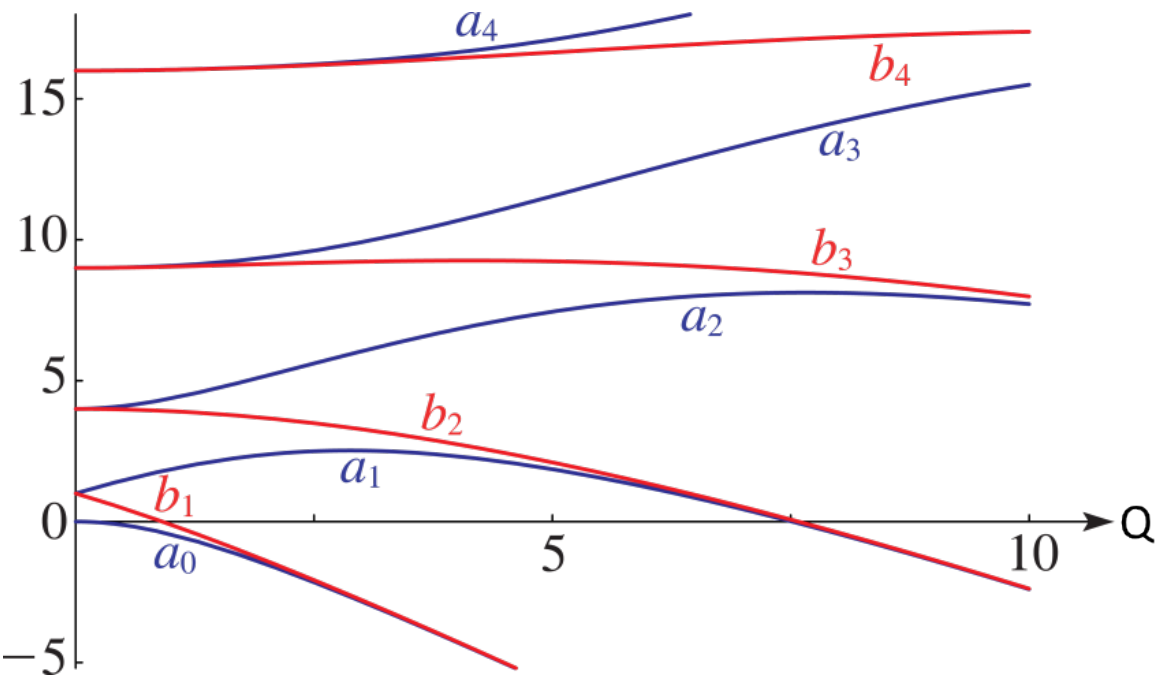

Figure 2.2: Mathieu integer eigenvalues for $0 \leq Q \leq 10$ [22, Fig. 28.2.1].

These functions form an orthogonal basis set over 2π with normalization $1/\sqrt{\pi}$. That is:

$$\begin{aligned} &\int_0^{2\pi} ce_m(\tilde{z}) ce_n(\tilde{z}) d\tilde{z} = \int_0^{2\pi} se_m(\tilde{z}) se_n(\tilde{z}) d\tilde{z} = 0 \quad : \quad m \neq n \\ &\int_0^{2\pi} se_m(\tilde{z}) ce_n(\tilde{z}) d\tilde{z} = 0 \end{aligned} \tag{2.18}$$

and

$$\int_0^{2\pi} (ce_n(\tilde{z}))^2 = \int_0^{2\pi} (se_n(\tilde{z}))^2 = \pi \tag{2.19}$$

As an aside, we may note that for $Q = 0$ these solutions reduce to the FFG problem where:

$$ce_0(\tilde{z}, 0) = \frac{1}{\sqrt{2}} \quad , \quad ce_n(\tilde{z}, 0) = \cos(n\tilde{z}) \quad , \quad se_n(\tilde{z}, 0) = \sin(n\tilde{z}) \quad : \quad n = 0, 1, 2, \ldots \tag{2.20}$$

and

$$a_n(0) = n^2 \quad , \quad b_m(0) = m^2 \quad : \quad n = 0, 1, 2, \ldots \quad , \quad m = 1, 2, 3, \ldots \tag{2.21}$$

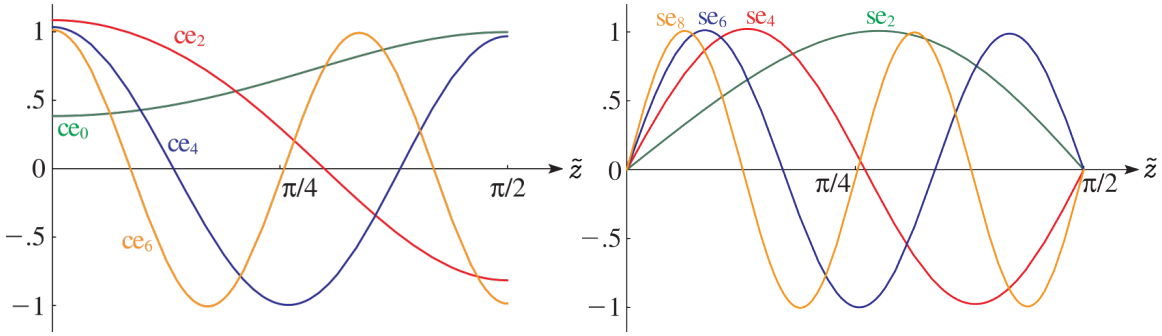

Figure 2.3: Mathieu even and odd π-periodic eigenfunctions for $Q = 1$ [22, Fig. 28.3.1, 28.3.7].

This relationship between the FFG and the Mathieu Fermi gas (MFG) displays an important feature in the enumeration of degenerate eigenstates. We note that in the FFG, for $n \geq 1 : a_n = b_n = n^2$ and there is a twofold degeneracy of the eigenvalue n^2 corresponding to two wavevectors with components (n_x, n_y, n) and $(n_x, n_y, -n)$. However, when moving to the MFG with $Q > 0$ this degeneracy is broken, as shown by the bifurcation of the $n \geq 1$ eigenvalues in Fig. (2.2). Additionally, we are still able to assign a n_z quantum number to the solutions as they have well ordered eigenvalues for all Q. That is, we assign $n_z = 0 \to a_0$, $n_z = 1 \to b_1$, $n_z = 2 \to a_1$, ...

We can finally see that we are able to construct a complete, orthonormal basis set of eigenfunctions with corresponding eigenenergies for the MFG system. The even solutions are (for $n_z = 0, 2, 4, \dots$):

$$\phi_i(\mathbf{r}) = \frac{1}{L\sqrt{\pi}} e^{i(k_x x + k_y y)} ce_{n_z}(q, qz/2) \quad , \quad e_i(k_x, k_y, q) = \frac{\hbar^2}{2m}\left[k_x^2 + k_y^2 + \left(\frac{q}{2}\right)^2 a_{n_z}(q)\right] \tag{2.22}$$

and the odd solutions (for $n_z = 1, 3, 5, \dots$):

$$\phi_i(\mathbf{r}) = \frac{1}{L\sqrt{\pi}} e^{i(k_x x + k_y y)} se_{n_z}(q, qz/2) \quad , \quad e_i(k_x, k_y, q) = \frac{\hbar^2}{2m}\left[k_x^2 + k_y^2 + \left(\frac{q}{2}\right)^2 b_{n_z}(q)\right] \tag{2.23}$$

We note that the k_x, k_y are simply the one dimensional FFG wavenumbers with the usual properties.

Using these solutions, we are able to compute the energy per particle in the MFG system. We calculate these at a density of 0.10 fm^{-3}, external potential strengths of v_q = 0.0, 0.05, 0.10, 0.15, 0.20, 0.25, 0.30, 0.35, 0.40, 0.45 and 0.50 times E_F with q = 0.25, 0.50, 0.75, 1, 1.5, 2 and 2.5 times $2\pi/L$ for the 66 particle system and q = 1, 2, 3, 4, 6, 8, 12, 16, 24, 32 and 40 times $2\pi/L$ for the 4224 particle system. In both cases, L is the the length of the box containing 4224 particles to ensure an integer number of periods fits in each box. These energies were used to calculate the linear density-density response functions and have been compared to the TL response function for the Fermi gas which is given by the Lindhard function in Fig. (2.4). The Lindhard function is:

$$\chi_L = -\frac{mq_F}{2\pi^2\hbar^2}\left[1 + \frac{q_F}{q}\left(1 - \left(\frac{q}{2q_F}\right)^2\right)\ln\left|\frac{q + 2q_F}{q - 2q_F}\right|\right] \tag{2.24}$$

It is immediately apparent that both the 66 and 4224 particle cases agree well

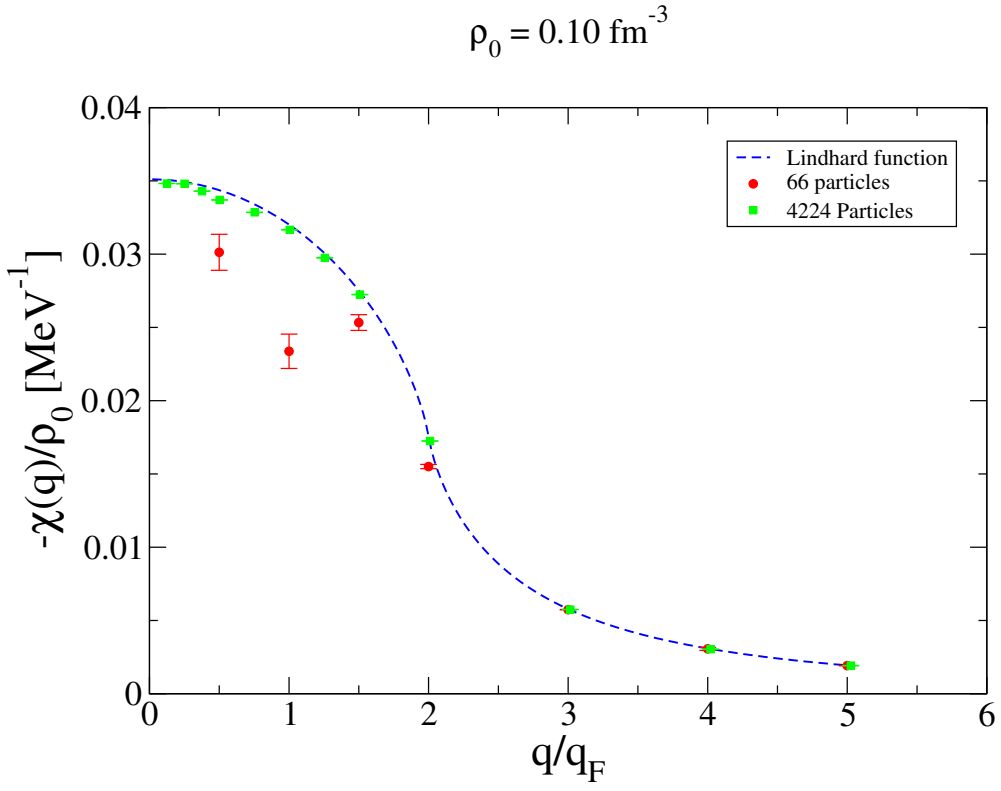

Figure 2.4: Finite size effects on static response functions for 66 and 4224 particle MFG systems at a density of $\rho = 0.10 fm^{-3}$. The Lindhard function is the TL static response function for the MFG.

for $q/q_F \geq 3$. However, significant errors due to finite size effects are incurred in the 66 particle case below this threshold, whereas the 4224 particle case has relatively minor error across the entire spectrum. We can see in Table 2.1, the maximum error in the 4224 particle case is 1.92% at $q/q_F \approx 0.5$ with the 66 particle case having a maximum error of 26.9% at $q/q_F \approx 1$. These errors due to finite size effects in the 4224 particle case are of the same order as the error that will be incurred due to the solution techniques used in the next section. As such, we are assured that studying the 4224 particle case will be sufficient as a model for the case in the TL with the assumptions that will follow.

Table 2.1: The relative percent error due to finite size effects for 66 and 4224 particles at a density of 0.10 fm^{-3}

q/q_F	0.503	1.005	1.508	2.010	3.015	4.021	5.023
66 Particle %Error	12.3%	26.9%	7.63%	8.89%	0.41%	0.12%	0.14%
4224 Particle %Error	1.92%	1.01%	0.67%	1.36%	0.57%	0.45%	0.19%

Chapter 3

Numerical Methods

3.1 Hartree-Fock Equations

We first consider the previously discussed energy density functional $\mathcal{H}(\mathbf{r})$ for infinite neutron matter in the presence of an external potential $v(z)$ along the z-axis. In its most general form, this energy density functional will take the form [20]:

$$\begin{aligned}\mathcal{H}(\mathbf{r}) = &\frac{\hbar^2}{2m}\tau(\mathbf{r}) + \frac{1}{4}t_0(1-x_0)\rho^2(\mathbf{r}) + \frac{1}{24}t_3(1-x_3)\rho^{2+\alpha}(\mathbf{r}) \\ &+ \frac{1}{8}\big[t_1(1-x_1) + 3t_2(1+x_2)\big]\rho(\mathbf{r})\tau(\mathbf{r}) \\ &+ \frac{3}{32}\big[t_1(1-x_1) - t_2(2+x_2)\big]\big(\nabla\rho(\mathbf{r})\big)^2 + W_0\mathbf{J}(\mathbf{r})\cdot\nabla\rho(\mathbf{r}) \\ &+ \big[t_1(1-x_1) - t_2(1+x_2)\big]\mathbf{J}^2(\mathbf{r}) + v(z)\rho(\mathbf{r}) \end{aligned} \tag{3.1}$$

In the case of infinite neutron matter, a spin saturated system, we find that the effects of the spin density terms $\mathbf{J}(\mathbf{r})$ are vanishing, and in a smaller system such as ^{208}Pb will only contribute to $\sim 0.4\%$ of the total binding energy [23, 20]. Thus, even in the case of a finite box simulation with nonzero spin density terms, we are free to rewrite

the energy density functional with only a small loss of generality as:

$$\begin{aligned}\mathcal{H}(\mathbf{r}) = &\frac{\hbar^2}{2m}\tau(\mathbf{r}) + \frac{1}{4}t_0(1-x_0)\rho^2(\mathbf{r}) + \frac{1}{24}t_3(1-x_3)\rho^{2+\alpha}(\mathbf{r}) \\ &+ \frac{1}{8}\big[t_1(1-x_1) + 3t_2(1+x_2)\big]\rho(\mathbf{r})\tau(\mathbf{r}) \\ &+ \frac{3}{32}\big[t_1(1-x_1) - t_2(2+x_2)\big]\big(\nabla\rho(\mathbf{r})\big)^2 + v(z)\rho(\mathbf{r}) \end{aligned} \tag{3.2}$$

From the energy density functional, we would like to find the ground state of the infinite neutron system. This is obtained by considering the total energy E that remains stationary under the variation of the single particle wavefunctions ϕ_i [19]. This is equivalent to the expression:

$$\frac{\delta}{\delta\phi_i}\Big(E - \sum_j e_j \int d\mathbf{r}|\phi_j(\mathbf{r})|^2\Big) = \frac{\delta}{\delta\phi_i}\Big(\int d\mathbf{r}\mathcal{H}(\mathbf{r}) - \sum_j e_j \int d\mathbf{r}|\phi_j(\mathbf{r})|^2\Big) = 0 \tag{3.3}$$

where the e_j are the single particle variational parameters, which will later turn out to be the single particle energies. To solve this we consider both terms of this expression:

$$\frac{\delta}{\delta\phi_i}\sum_j e_j \int d\mathbf{r}|\phi_j(\mathbf{r})|^2 = \sum_j e_j \int d\mathbf{r}\frac{\delta}{\delta\phi_i}\big(\phi_j^*(\mathbf{r})\phi_j(\mathbf{r})\big) \tag{3.4}$$

and

$$\begin{aligned}\frac{\delta}{\delta\phi_i}\int d\mathbf{r}\mathcal{H}(\mathbf{r}) = &\int d\mathbf{r}\Bigg\{\frac{\hbar^2}{2m}\frac{\delta}{\delta\phi_i}\tau(\mathbf{r}) + \frac{1}{4}t_0(1-x_0)\frac{\delta}{\delta\phi_i}\rho^2(\mathbf{r}) + \frac{1}{24}t_3(1-x_3)\frac{\delta}{\delta\phi_i}\rho^{2+\alpha}(\mathbf{r}) \\ &+ \frac{1}{8}\big[t_1(1-x_1) + 3t_2(1+x_2)\big]\frac{\delta}{\delta\phi_i}\big[\rho(\mathbf{r})\tau(\mathbf{r})\big] \\ &+ \frac{3}{32}\big[t_1(1-x_1) - t_2(2+x_2)\big]\frac{\delta}{\delta\phi_i}\big[\nabla\rho(\mathbf{r})\big]^2 + v(z)\frac{\delta}{\delta\phi_i}\rho(\mathbf{r})\Bigg\} \\ = &\int d\mathbf{r}\Bigg\{\frac{\hbar^2}{2m}\frac{\delta}{\delta\phi_i}\tau(\mathbf{r}) + \frac{1}{2}t_0(1-x_0)\rho(\mathbf{r})\frac{\delta}{\delta\phi_i}\rho(\mathbf{r}) \\ &+ \frac{2+\alpha}{24}t_3(1-x_3)\rho^{1+\alpha}(\mathbf{r})\frac{\delta}{\delta\phi_i}\rho(\mathbf{r})\end{aligned}$$

$$+\frac{1}{8}\big[t_1(1-x_1)+3t_2(1+x_2)\big]\left[\rho(\mathbf{r})\frac{\delta}{\delta\phi_i}\tau(\mathbf{r})+\tau(\mathbf{r})\frac{\delta}{\delta\phi_i}\rho(\mathbf{r})\right]$$
$$+\frac{3}{16}\big[t_1(1-x_1)-t_2(2+x_2)\big]\nabla\rho(\mathbf{r})\frac{\delta}{\delta\phi_i}\nabla\rho(\mathbf{r})+v(z)\frac{\delta}{\delta\phi_i}\rho(\mathbf{r})\Bigg\} \tag{3.5}$$

Paying additional consideration to the term dependent on $\nabla\rho(\mathbf{r})$, we integrate by parts to recover a more tractable form.

$$\int d\mathbf{r}\nabla\rho(\mathbf{r})\frac{\delta}{\delta\phi_i}\nabla\rho(\mathbf{r})=\nabla\rho(\mathbf{r})\frac{\delta}{\delta\phi_i}\rho(\mathbf{r})\Big|_\Omega-\int d\mathbf{r}\nabla^2\rho(\mathbf{r})\frac{\delta}{\delta\phi_i}\rho(\mathbf{r})=-\int d\mathbf{r}\nabla^2\rho(\mathbf{r})\frac{\delta}{\delta\phi_i}\rho(\mathbf{r}) \tag{3.6}$$

We note that from the principles of the calculus of variations, the term $\frac{\delta}{\delta\phi_i}\rho(\mathbf{r})$ must be vanishing at the boundary, denoted by Ω, as the single particle wavefunctions $\phi_i(\mathbf{r})$ are held fixed at these points. Thus, we may now rewrite Eq. (3.5) in the compact form:

$$\begin{aligned}\frac{\delta}{\delta\phi_i}\int d\mathbf{r}\mathcal{H}(\mathbf{r}) &= \int d\mathbf{r}\Bigg(\left\{\frac{\hbar^2}{2m}+\frac{1}{8}\big[t_1(1-x_1)+3t_2(1+x_2)\big]\right\}\frac{\delta}{\delta\phi_i}\tau(\mathbf{r})\\
&+\Bigg\{\frac{1}{2}t_0(1-x_0)\rho(\mathbf{r})+\frac{2+\alpha}{24}t_3(1-x_3)\rho^{1+\alpha}(\mathbf{r})\\
&+\frac{1}{8}\big[t_1(1-x_1)+3t_2(1+x_2)\big]\tau(\mathbf{r})\\
&-\frac{3}{16}\big[t_1(1-x_1)-t_2(2+x_2)\big]\nabla^2\rho(\mathbf{r})+v(z)\Bigg\}\frac{\delta}{\delta\phi_i}\rho(\mathbf{r})\Bigg)\\
&=\int d\mathbf{r}\left(\frac{\hbar^2}{2m^*(\mathbf{r})}\frac{\delta}{\delta\phi_i}\tau(\mathbf{r})+U(\mathbf{r})\frac{\delta}{\delta\phi_i}\rho(\mathbf{r})+v(z)\frac{\delta}{\delta\phi_i}\rho(\mathbf{r})\right)\end{aligned} \tag{3.7}$$

Where we define the effective mass term:

$$\frac{\hbar^2}{2m^*(\mathbf{r})}=\frac{\hbar^2}{2m}+\frac{1}{8}\big[t_1(1-x_1)+3t_2(1+x_2)\big] \tag{3.8}$$

and the interaction potential term:

$$U(\mathbf{r}) = \frac{1}{2}t_0(1-x_0)\rho(\mathbf{r}) + \frac{2+\alpha}{24}t_3(1-x_3)\rho^{1+\alpha}(\mathbf{r}) + \frac{1}{8}\big[t_1(1-x_1)+3t_2(1+x_2)\big]\tau(\mathbf{r}) - \frac{3}{16}\big[t_1(1-x_1)-t_2(2+x_2)\big]\nabla^2\rho(\mathbf{r}) \tag{3.9}$$

Recalling the definitions of the density and kinetic density, we are able to calculate the variations with respect to the single particle wavefunctions of these terms [19].

$$\frac{\delta}{\delta\phi_i}\rho(\mathbf{r}) = \frac{\delta}{\delta\phi_i}\sum_j \big|\phi_j(\mathbf{r})\big|^2 = \sum_j \frac{\delta}{\delta\phi_i}\big(\phi_j^*(\mathbf{r})\phi_j(\mathbf{r})\big) = 2\sum_j \phi_j(\mathbf{r})\frac{\delta}{\delta\phi_i}\phi_j^*(\mathbf{r}) \tag{3.10}$$

$$\frac{\delta}{\delta\phi_i}\tau(\mathbf{r}) = \frac{\delta}{\delta\phi_i}\sum_j \big|\nabla\phi_j(\mathbf{r})\big|^2 = \sum_j \frac{\delta}{\delta\phi_i}\big(\nabla\phi_j^*(\mathbf{r})\cdot\nabla\phi_j(\mathbf{r})\big) = 2\sum_j \nabla\phi_j(\mathbf{r})\cdot\frac{\delta}{\delta\phi_i}\nabla\phi_j^*(\mathbf{r}) \tag{3.11}$$

Using this form for the variational derivative of the kinetic density $\tau(\mathbf{r})$, we may integrate the first component of the right hand side of Eq. (3.7) by parts.

$$\begin{aligned}\int d\mathbf{r}\frac{\hbar^2}{2m^*(\mathbf{r})}\frac{\delta}{\delta\phi_i}\tau(\mathbf{r}) &= 2\sum_j\int d\mathbf{r}\frac{\hbar^2}{2m^*(\mathbf{r})}\nabla\phi_j(\mathbf{r})\cdot\frac{\delta}{\delta\phi_i}\nabla\phi_j^*(\mathbf{r}) \\ &= 2\sum_j\left[\frac{\hbar^2}{2m^*(\mathbf{r})}\nabla\phi_j(\mathbf{r})\frac{\delta}{\delta\phi_i}\phi_j^*(\mathbf{r})\Big|_\Omega\right. \\ &\quad \left. - \int d\mathbf{r}\left(\frac{\delta}{\delta\phi_i}\phi_j^*(\mathbf{r})\right)\nabla\cdot\left(\frac{\hbar^2}{2m^*(\mathbf{r})}\nabla\phi_j(\mathbf{r})\right)\right] \\ &= -2\sum_j\int d\mathbf{r}\left(\frac{\delta}{\delta\phi_i}\phi_j^*(\mathbf{r})\right)\nabla\cdot\left(\frac{\hbar^2}{2m^*(\mathbf{r})}\nabla\phi_j(\mathbf{r})\right)\end{aligned} \tag{3.12}$$

Where we again find that $\frac{\delta}{\delta\phi_i}\phi_j^*(\mathbf{r})$ is vanishing on the boundary Ω since the single particle wavefunctions $\phi_i(\mathbf{r})$ are fixed at those points. Thus, we may now combine

these new derivations and insert them into Eq. (3.3) to find:

$$2\sum_j \int d\mathbf{r} \frac{\delta}{\delta\phi_i}\phi_j^*(\mathbf{r})\left[-\nabla\cdot\left(\frac{\hbar^2}{2m^*(\mathbf{r})}\nabla\phi_j(\mathbf{r})\right) + U(\mathbf{r})\phi_j(\mathbf{r}) + v(z)\phi_j(\mathbf{r}) - e_j\phi_j(\mathbf{r})\right] = 0 \tag{3.13}$$

For this expression to be equal to zero, it is required that the integrand is equal to zero for all $\mathbf{r}$, and we will recover the Hartree-Fock equations governing the single particle states in infinite neutron matter in the presence of an external potential $v(z)$.

$$-\nabla\cdot\left(\frac{\hbar^2}{2m^*(\mathbf{r})}\nabla\phi_j(\mathbf{r})\right) + U(\mathbf{r})\phi_j(\mathbf{r}) + v(z)\phi_j(\mathbf{r}) = e_j\phi_j(\mathbf{r}) \tag{3.14}$$

In infinite neutron matter, we will find that in the absence of an external potential, the density and kinetic energy density must be homogeneous and isotropic throughout due to the symmetry of the system. However, with the addition of the external potential along the z-axis this symmetry will broken and we will find that the density and kinetic energy densities must now be only dependent on the z-coordinate.

$$\rho(\mathbf{r}) = \rho(z) \quad , \quad \tau(\mathbf{r}) = \tau(z) \tag{3.15}$$

Noticing that the effective mass term Eq. (3.8) and the interaction potential term Eq. (3.9) only depend on $\mathbf{r}$ through the density and kinetic density functions, we will again observe that these terms are also dependent only on the z-coordinate.

$$\frac{\hbar^2}{2m^*(\mathbf{r})} = \frac{\hbar^2}{2m^*(z)} \quad , \quad U(\mathbf{r}) = U(z) \tag{3.16}$$

Expanding the Hartree-Fock equations and collecting terms produces a second order linear partial differential equation:

$$-\frac{\hbar^2}{2m^*(z)}\nabla^2\phi_i(\mathbf{r}) - \left(\nabla\frac{\hbar^2}{2m^*(z)}\right)\cdot\nabla\phi_i(\mathbf{r}) + \Big(U(z) + v(z) - e_i\Big)\phi_i(\mathbf{r}) = 0 \tag{3.17}$$

We can see that since all of the coefficient functions are strictly dependent on only the z-coordinate, it is possible to employ the separation of variables method to solve this equation by decomposing the single particle wavefunction into the form:

$$\phi_i(\mathbf{r}) = \phi_{i,x}(x)\phi_{i,y}(y)\phi_{i,z}(z) \tag{3.18}$$

Substituting this expression into the Eq. (3.17) produces the expression:

$$\begin{aligned}
&-\frac{\hbar^2}{2m^*(z)}\Big(\phi_{i,y}(y)\phi_{i,z}(z)\frac{d^2}{dx^2}\phi_{i,x}(x) + \phi_{i,x}(x)\phi_{i,z}(z)\frac{d^2}{dy^2}\phi_{i,y}(y) + \phi_{i,x}(x)\phi_{i,y}(y)\frac{d^2}{dz^2}\phi_{i,z}(z)\Big) \\
&-\Big(\hat{z}\frac{d}{dz}\frac{\hbar^2}{2m^*(z)}\Big)\cdot\Big(\hat{x}\phi_{i,y}(y)\phi_{i,z}(z)\frac{d}{dx}\phi_{i,x}(x) + \hat{y}\phi_{i,x}(x)\phi_{i,z}(z)\frac{d}{dy}\phi_{i,y}(y) + \hat{z}\phi_{i,x}(x)\phi_{i,y}(y)\frac{d}{dz}\phi_{i,z}(z)\Big) \\
&+\Big(U(z) + v(z) - e_i\Big)\phi_{i,x}(x)\phi_{i,y}(y)\phi_{i,z}(z) \\
&=-\frac{\hbar^2}{2m^*(z)}\Big(\phi_{i,y}(y)\phi_{i,z}(z)\frac{d^2}{dx^2}\phi_{i,x}(x) + \phi_{i,x}(x)\phi_{i,z}(z)\frac{d^2}{dy^2}\phi_{i,y}(y) + \phi_{i,x}(x)\phi_{i,y}(y)\frac{d^2}{dz^2}\phi_{i,z}(z)\Big) \\
&-\Big(\frac{d}{dz}\frac{\hbar^2}{2m^*(z)}\Big)\cdot\Big(\phi_{i,x}(x)\phi_{i,y}(y)\frac{d}{dz}\phi_{i,z}(z)\Big) + \Big(U(z) + v(z) - e_i\Big)\phi_{i,x}(x)\phi_{i,y}(y)\phi_{i,z}(z)
\end{aligned}$$

Where we note that we made the substitution

$$\nabla\frac{\hbar^2}{2m_n^*(z)} = \hat{z}\frac{d}{dz}\frac{\hbar^2}{2m^*(z)} \tag{3.19}$$

as the effective mass term is only dependent on the z coordinate. Dividing through by $-\frac{\hbar^2}{2m_n^*(z)}\phi_i(\mathbf{r})$produces the following equation:

$$\frac{\frac{d^2}{dx^2}\phi_{i,x}(x)}{\phi_{i,x}(x)} + \frac{\frac{d^2}{dy^2}\phi_{i,y}(y)}{\phi_{i,y}(y)} + \frac{\frac{d^2}{dz^2}\phi_{i,z}(z)}{\phi_{i,z}(z)} + \left(\frac{\frac{d}{dz}\frac{\hbar^2}{2m^*(z)}}{\frac{\hbar^2}{2m^*(z)}}\right)\frac{\frac{d}{dz}\phi_{i,z}(z)}{\phi_{i,z}(z)} - \frac{U(z) + v(z) - e_i}{\frac{\hbar^2}{2m^*(z)}} = 0 \tag{3.20}$$

Thus, the Hartree-Fock equations have been recast to a form such that all coordinate dependencies are decoupled. Continuing in the usual manner to solve partial differential equations, we separate the wavefunctions for each coordinate into a set of

decoupled ordinary differential equations as follows:

$$\frac{\frac{d^2}{dx^2}\phi_{i,x}(x)}{\phi_{i,x}(x)} = -k_x^2 = -\frac{\frac{d^2}{dy^2}\phi_{i,y}(y)}{\phi_{i,y}(y)} - \frac{\frac{d^2}{dz^2}\phi_{i,z}(z)}{\phi_{i,z}(z)} - \left(\frac{\frac{d}{dz}\frac{\hbar^2}{2m^*(z)}}{\frac{\hbar^2}{2m^*(z)}}\right)\frac{\frac{d}{dz}\phi_{i,z}(z)}{\phi_{i,z}(z)} + \frac{U(z)+v(z)-e_i}{\frac{\hbar^2}{2m^*(z)}} \tag{3.21}$$

$$\frac{\frac{d^2}{dy^2}\phi_{i,y}(y)}{\phi_{i,y}(y)} = -k_y^2 = k_x^2 - \frac{\frac{d^2}{dz^2}\phi_{i,z}(z)}{\phi_{i,z}(z)} - \left(\frac{\frac{d}{dz}\frac{\hbar^2}{2m^*(z)}}{\frac{\hbar^2}{2m^*(z)}}\right)\frac{\frac{d}{dz}\phi_{i,z}(z)}{\phi_{i,z}(z)} + \frac{U(z)+v(z)-e_i}{\frac{\hbar^2}{2m^*(z)}} \tag{3.22}$$

$$\frac{\frac{d^2}{dz^2}\phi_{i,z}(z)}{\phi_{i,z}(z)} + \left(\frac{\frac{d}{dz}\frac{\hbar^2}{2m^*(z)}}{\frac{\hbar^2}{2m^*(z)}}\right)\frac{\frac{d}{dz}\phi_{i,z}(z)}{\phi_{i,z}(z)} - \frac{U(z)+v(z)-e_i}{\frac{\hbar^2}{2m^*(z)}} - k_x^2 - k_y^2 = 0 \tag{3.23}$$

Rewriting these ordinary differential equations into their standard forms reveals that both the x and y-axis equations are simply the wave equation where the constants of separation k_x and k_y are the wavenumbers to be determined by the boundary conditions of the system.

$$\frac{d^2}{dx^2}\phi_{i,x}(x) + k_x^2\phi_{i,x}(x) = 0 \tag{3.24}$$

$$\frac{d^2}{dy^2}\phi_{i,y}(y) + k_y^2\phi_{i,y}(y) = 0 \tag{3.25}$$

$$-\frac{\hbar^2}{2m^*(z)}\frac{d^2}{dz^2}\phi_{i,z}(z) - \left[\frac{d}{dz}\frac{\hbar^2}{2m^*(z)}\right]\frac{d}{dz}\phi_{i,z}(z) + \left[U(z)+v(z)+\frac{\hbar^2}{2m^*(z)}(k_x^2+k_y^2)\right]\phi_{i,z}(z)$$
$$= e_i\phi_{i,z}(z) \tag{3.26}$$

The general form of the solutions to both Eq. (3.24) and Eq. (3.25) are:

$$\phi_{i,x}(x) = \alpha_x \exp[ik_x x] + \beta_x \exp[-ik_x x] \tag{3.27}$$

$$\phi_{i,y}(y) = \alpha_y \exp[ik_y y] + \beta_y \exp[-ik_y y] \tag{3.28}$$

For infinite neutron matter, to obtain an accurate description of the dynamics, we simulate a sufficiently large enough subsystem contained in a finite periodic box of volume L^3. This condition imposes the standard periodic boundary conditions:

$$\phi_{i,x}(x) = \phi_{i,x}(x+L) \quad , \quad \phi_{i,y}(y) = \phi_{i,y}(y+L) \quad , \quad \phi_{i,z}(z) = \phi_{i,z}(z+L) \tag{3.29}$$

From these boundary conditions, we state the wavenumbers k_x and k_y from the general solution to the wave equation

$$k_x = \frac{2\pi n_x}{L} \quad , \quad k_y = \frac{2\pi n_y}{L} \tag{3.30}$$

where both $n_{i,x},\ n_{i,y} \in \mathbb{Z}$. To satisfy orthonormality conditions that will later be discussed, we state that the solutions

$$\phi_{i,x}(x) = \frac{1}{\sqrt{L}} \exp\left[\frac{2i\pi n_x}{L} x\right] \tag{3.31}$$

and

$$\phi_{i,y}(y) = \frac{1}{\sqrt{L}} \exp\left[\frac{2i\pi n_y}{L} y\right] \tag{3.32}$$

provide complete orthonormal basis sets for the x- and y-axis component wavefunctions.

3.2 Finite Difference Schemes

In our attempt to solve the complete nuclear many body problem for infinite neutron matter we must first consider the numerical methods to be used in computing the single particle wavefunctions and energies. In our case, this reduces to solving a second order linear ordinary differential equation with periodic boundary conditions, given by Eq. (3.26). The most general form for this type of equation, with eigenvalues e_i and eigenvectors $\phi_i(z)$ in a periodic box of length L, is:

$$A(z)\phi_i^{''}(z) + B(z)\phi_i^{'}(z) + C(z)\phi_i(z) = e_i\phi_i(z) \quad : \quad \phi_i(z) = \phi_i(z+L) \tag{3.33}$$

The initial, and seemingly simplest, solution techniques attempted utilized the fourth order Runge-Kutta method [24] and Numerov's method [25] paired with the shooting method for matching boundary conditions. Both of these techniques are iterative methods relying on a fixed initial condition $\phi_i(0)$ alongside an estimated eigenvalue E_i. The shooting method relies on this initial estimate to produce the end-point $\phi_i(L, E_i)$. We may use these estimates to generate the function $\Delta\phi_i(L, E_i) = \phi_i(0) - \phi_i(L, E_i)$ where some roots correspond to satisfying the periodic boundary condition. While valid methods, both Runge-Kutta and Numerov posed two significant problems. The first and most important of which was the increasing difficulty in finding the eigenvalues of excited states, where these eigenvalue roots become more densely packed and required significantly many more iterations in a root-finding method to be able to properly discern. The second problem was that since these methods were iterative, the accuracy of the solution $\phi_i(z)$ decreases with increasing z and adds a net bias to every single particle solution generated. For these reasons, both of these techniques were discarded in favour of the more robust finite difference method.

Before outlining the finite difference method, we would first like to convert our

general ordinary differential equation to a simpler form. We define a new wavefunction φ_i in terms of ϕ_i in the following manner [26]:

$$\varphi_i(z) = \Phi(z)\phi_i(z) \tag{3.34}$$

where $\Phi(z)$ is defined as:

$$\Phi(z) = \exp\left(\frac{1}{2}\int^z dsR(s)\right) \quad : \quad R(s) = \frac{B(s)}{A(s)} \tag{3.35}$$

Computing the first and second derivatives of φ_i produce:

$$\varphi_i^{'}(z) = \frac{1}{2}R(z)\Phi(z)\phi_i + \Phi(z)\phi_i^{'}(z) \tag{3.36}$$

and

$$\begin{aligned}
\varphi_i^{''}(z) &= \frac{1}{2}R^{'}(z)\Phi(z)\phi_i(z) + \frac{1}{4}R^2(z)\Phi(z)\phi_i(z) + \frac{1}{2}R(z)\Phi(z)\phi_i^{'}(z) \\
&+ \frac{1}{2}R(z)\Phi(z)\phi_i^{'}(z) + \Phi(z)\phi_i^{''}(z) \\
&= \Big(\frac{1}{2}R^{'}(z) + \frac{1}{4}R^2(z)\Big)\Phi(z)\phi_i(z) + R(z)\Phi(z)\phi_i^{'}(z) + \Phi(z)\phi_i^{''}(z)
\end{aligned} \tag{3.37}$$

Multiplying the second derivative term by the coefficient $A(z)$ produces the equation:

$$\begin{aligned}
A(z)\varphi_i^{''}(z) &= A(z)\Big(\frac{1}{2}R^{'}(z) + \frac{1}{4}R^2(z)\Big)\Phi(z)\phi_i(z) + \Phi(z)\Big(A(z)\phi_i^{''}(z) + A(z)R(z)\phi_i^{'}(z)\Big) \\
&= A(z)\Big(\frac{1}{2}R^{'}(z) + \frac{1}{4}R^2(z)\Big)\varphi_i(z) + \Phi(z)\Big(A(z)\phi_i^{''}(z) + B(z)\phi_i^{'}(z)\Big) \\
&= A(z)\Big(\frac{1}{2}R^{'}(z) + \frac{1}{4}R^2(z)\Big)\varphi_i(z) + \Phi(z)\Big(E_i - C(z)\Big)\phi_i(z) \\
&= D(z)\varphi_i(z) + \Big(E_i - C(z)\Big)\varphi_i(z)
\end{aligned} \tag{3.38}$$

$$\tag{3.39}$$

where we have made the definition:

$$D(z) = C(z) - A(z)\Big(\frac{1}{2}R^{'}(z) + \frac{1}{4}R^{2}(z)\Big) \tag{3.40}$$

It is now possible to rearrange Eq. (3.39) to take the form of a second order ordinary differential equation without a first derivative term $\varphi_i^{\prime}(z)$ as follows:

$$A(z)\varphi_i^{''}(z) + D(z)\varphi_i(z) = e_i\varphi_i \quad : \quad \varphi_i(z) = \varphi_i(z+L) \tag{3.41}$$

Thus, we have produced a simplified ordinary differential equation sharing eigenvalues E_i and eigenfunctions ϕ_i under the continuous change of variable $\Phi(z)$ with Eq. (3.33). This process of removing the first derivative term was carried out in order to optimize the solution techniques that will be used further on.

With the prepared ordinary differential equation Eq. (3.41), we are able to construct the corresponding finite difference scheme [25]. The first step in this construction is to discretize the space that our solution will be valid in. For a periodic box of length L, we provide a discretization of the wavefunction $\varphi_i(z)$:

$$\boldsymbol{\varphi}_i = \begin{pmatrix} \varphi_i^0 \\ \\ \vdots \\ \\ \varphi_i^{N-1} \end{pmatrix} \tag{3.42}$$

where we have defined:

$$\varphi_i^j = \varphi_i(j\Delta z) \quad : \quad \Delta z = \frac{L}{N} \tag{3.43}$$

where N is the number of points used to generate the scheme, and will correspond

to an error of order $\mathcal{O}(N^{-4})$. With the basic discretization scheme in place, a 5 point stencil is used to approximate the second derivative $\varphi_i^{''}(z)$. To produce the 5 point stencil, we consider the Taylor series for $\varphi_i(z \pm \Delta z)$ and $\varphi_i(z \pm 2\Delta z)$. It is straightforward to find:

$$\varphi_i(z \pm \Delta z) = \varphi_i(z) \pm \Delta z \varphi_i^{'}(z) + \frac{\Delta z^2}{2}\varphi_i^{''}(z) \pm \frac{\Delta z^3}{3}\varphi_i^{'''}(z) + \mathcal{O}(\Delta z^4) \tag{3.44}$$

$$\varphi_i(z \pm 2\Delta z) = \varphi_i(z) \pm 2\Delta z \varphi_i^{'}(z) + \frac{4\Delta z^2}{2}\varphi_i^{''}(z) \pm \frac{8\Delta z^3}{3}\varphi_i^{'''}(z) + \mathcal{O}(\Delta z^4) \tag{3.45}$$

Using these expressions, we rearrange and solve for the centered finite difference schemes for $\varphi_i^{''}(z)$.

$$\varphi_i^{''}(z) \approx \frac{-\varphi_i(z+2\Delta z) + 16\varphi_i(z+\Delta z) - 30\varphi_i(z) + 16\varphi_i(z-\Delta z) - \varphi_i(z-2\Delta z)}{12\Delta z^2} + \mathcal{O}(\Delta z^4) \tag{3.46}$$

We can now begin to see the benefit of recasting Eq. (3.33) to a form without a first derivative, as the second derivative term is symmetric under sign inversion of Δz whereas the first derivative term does not share this property. Since we only require the second derivative, it may be rewritten in terms of the discretized wavefunction $\boldsymbol{\varphi}_i$ and will take the form:

$$\varphi_i^{j''} \approx \frac{-\varphi_i^{j+2} + 16\varphi_i^{j+1} - 30\varphi_i^{j} + 16\varphi_i^{j-1} - \varphi_i^{j-2}}{12\Delta z^2} + \mathcal{O}(\Delta z^4) \tag{3.47}$$

It is now possible to rewrite Eq. (3.41) in the discretized form:

$$A^j \varphi_i^{j''} + D^j \varphi_i^j = E_i \varphi_i^j \quad : \quad A^j = A(j\Delta z) \quad , \quad D^j = D(j\Delta z) \tag{3.48}$$

Substituting the 5 point stencil approximation Eq. (3.47) for $\varphi_i^{j''}$ it is now immediately

apparent that this describes a matrix eigenvalue problem.

$$-\frac{A^j}{12\Delta z^2}\varphi_i^{j+2}+\frac{16A^j}{12\Delta z^2}\varphi_i^{j+1}+\Big(D^j-\frac{30A^j}{12\Delta z^2}\Big)\varphi_i^j+\frac{16A^j}{12\Delta z^2}\varphi_i^{j-1}-\frac{A^j}{12\Delta z^2}\varphi_i^{j-2}=e_i\varphi_i^j \tag{3.49}$$

For simplicity, we make the redefinitions:

$$\tilde{A}^j=\frac{A^j}{12\Delta z^2} \quad , \quad \tilde{D}^j=D^j-30\tilde{A}^j \tag{3.50}$$

so that Eq. (3.49) can be rewritten as:

$$-\tilde{A}^j\varphi_i^{j+2}+16\tilde{A}^j\varphi_i^{j+1}+\tilde{D}^j\varphi_i^j+16\tilde{A}^j\varphi_i^{j-1}-\tilde{A}^j\varphi_i^{j-2}=e_i\varphi_i^j \tag{3.51}$$

At this point, we impose the periodic boundary conditions at the endpoints for the box of length L. That is,

$$\varphi_i(0)=\varphi_i(L) \qquad , \qquad \varphi_i'(0)=\varphi_i'(L) \tag{3.52}$$

Translating these periodic boundary conditions into their discretized forms, and using the appropriate five point stencils gives the following set of equations:
For $\varphi_i(0)=\varphi_i(L)$:

$$\varphi_i(0)=\varphi(N\Delta z) \implies \varphi_i^0=\varphi_i^N \tag{3.53}$$

For $\varphi_i'(0)=\varphi_i'(L)$:

$$\begin{aligned}
&\varphi_i(-\Delta z)=\varphi((N-1)\Delta z) \implies \varphi_i^{-1}=\varphi_i^{N-1}\\
&\varphi_i(-2\Delta z)=\varphi((N-2)\Delta z) \implies \varphi_i^{-2}=\varphi_i^{N-2}\\
&\varphi_i(\Delta z)=\varphi((N+1)\Delta z) \implies \varphi_i^{1}=\varphi_i^{N+1}
\end{aligned}$$

$$\varphi_i(2\Delta z) = \varphi((N+2)\Delta z) \implies \varphi_i^2 = \varphi_i^{N+2} \tag{3.54}$$

Using these boundary conditions, the matrix equation Eq. (3.51) may be interpreted at the boundaries as follows:

$$\begin{aligned}
&-\tilde{A}^j\varphi_i^2 + 16\tilde{A}^j\varphi_i^1 + \tilde{D}^j\varphi_i^0 + 16\tilde{A}^j\varphi_i^{N-1} - \tilde{A}^j\varphi_i^{N-2} = e_i\varphi_i^0 \\
&-\tilde{A}^j\varphi_i^3 + 16\tilde{A}^j\varphi_i^2 + \tilde{D}^j\varphi_i^1 + 16\tilde{A}^j\varphi_i^0 - \tilde{A}^j\varphi_i^{N-1} = e_i\varphi_i^1 \\
&-\tilde{A}^j\varphi_i^1 + 16\tilde{A}^j\varphi_i^0 + \tilde{D}^j\varphi_i^{N-1} + 16\tilde{A}^j\varphi_i^{N-2} - \tilde{A}^j\varphi_i^{N-3} = e_i\varphi_i^{N-1} \\
&-\tilde{A}^j\varphi_i^0 + 16\tilde{A}^j\varphi_i^{N-1} + \tilde{D}^j\varphi_i^{N-2} + 16\tilde{A}^j\varphi_i^{N-3} - \tilde{A}^j\varphi_i^{N-4} = e_i\varphi_i^{N-2}
\end{aligned} \tag{3.55}$$

Using the above boundary equations Eq. (3.55) alongside the general matrix equation Eq. (3.51), we construct the matrix equation:

$$M\boldsymbol{\varphi}_i = e_i\boldsymbol{\varphi}_i \tag{3.56}$$

where the matrix, M, takes the form:

$$M = \begin{pmatrix} \tilde{D}_0 & 16\tilde{A}_0 & -\tilde{A}_0 & 0 & \cdots & 0 & -\tilde{A}_0 & 16\tilde{A}_0 \\ 16\tilde{A}_1 & \tilde{D}_1 & 16\tilde{A}_1 & -\tilde{A}_1 & 0 & \cdots & 0 & -\tilde{A}_1 \\ -\tilde{A}_2 & 16\tilde{A}_2 & \tilde{D}_2 & 16\tilde{A}_2 & -\tilde{A}_2 & 0 & \cdots & 0 \\ 0 & -\tilde{A}_3 & 16\tilde{A}_3 & \tilde{D}_3 & 16\tilde{A}_3 & -\tilde{A}_3 & 0 & \vdots \\ \vdots & \ddots & \ddots & \ddots & \ddots & \ddots & \ddots & \vdots \\ \vdots & 0 & -\tilde{A}_{N-4} & 16\tilde{A}_{N-4} & \tilde{D}_{N-4} & 16\tilde{A}_{N-4} & -\tilde{A}_{N-4} & 0 \\ 0 & \cdots & 0 & -\tilde{A}_{N-3} & 16\tilde{A}_{N-3} & \tilde{D}_{N-3} & 16\tilde{A}_{N-3} & -\tilde{A}_{N-3} \\ -\tilde{A}_{N-2} & 0 & \cdots & 0 & -\tilde{A}_{N-2} & 16\tilde{A}_{N-2} & \tilde{D}_{N-2} & 16\tilde{A}_{N-2} \\ 16\tilde{A}_{N-1} & -\tilde{A}_{N-1} & 0 & \cdots & 0 & -\tilde{A}_{N-1} & 16\tilde{A}_{N-1} & \tilde{D}_{N-1} \end{pmatrix} \tag{3.57}$$

Diagonalizing this matrix produces the complete orthonormal basis set

$$\{\boldsymbol{\varphi}_i, e_i\} \tag{3.58}$$

of the first N eigenvectors $\boldsymbol{\varphi}_i$ and corresponding eigenvalues e_i. We use the LAPACK (Linear Algebra Package) dgges function to compute the diagonalized form of this matrix which also guarantees the orthonormality of these calculated eigenvectors.

Recalling the transformation equations Eq. (3.34) and Eq. (3.35) we define the

discretized inverse transform matrix, which is immediately apparent to be invertible:

$$\boldsymbol{\Phi}^{-1} = \begin{pmatrix} \Phi_0^{-1} & 0 & \cdots & 0 \\ 0 & \ddots & 0 & \vdots \\ \vdots & 0 & \ddots & 0 \\ 0 & \cdots & 0 & \Phi_{N-1}^{-1} \end{pmatrix} \quad : \quad \Phi_j^{-1} = \exp\left(-\frac{1}{2} \int^{(j-1)\Delta z} dsR(s) \right) \tag{3.59}$$

This is used to recover the untransformed single particle eigenstates of the system $\boldsymbol{\phi}_i$.

$$\boldsymbol{\phi}_i = \boldsymbol{\Phi}^{-1} \boldsymbol{\varphi}_i \tag{3.60}$$

It is important to note that this transform preserves orthonormality as shown below:

$$\boldsymbol{\phi}_i^* \boldsymbol{\phi}_j = \left(\boldsymbol{\Phi}^{-1}\boldsymbol{\varphi}_i\right)^* \left(\boldsymbol{\Phi}^{-1}\boldsymbol{\varphi}_i\right) = \left(\boldsymbol{\varphi}_i^* \boldsymbol{\Phi}\right)\left(\boldsymbol{\Phi}^{-1}\boldsymbol{\varphi}_i\right) = \boldsymbol{\varphi}_i^* \left(\boldsymbol{\Phi}\boldsymbol{\Phi}^{-1}\right)\boldsymbol{\varphi}_i = \boldsymbol{\varphi}_i^* \boldsymbol{\varphi}_i = \delta_{ij} \tag{3.61}$$

Thus, we have constructed a system that accurately finds the first N eigenvalues e_i and discretized eigenvectors $\boldsymbol{\phi}_i$ for single particle differential eigenvalue equations in the form of Eq. (3.33).

3.3 Iterative Solution Techniques

Now we are finally able to use the solutions discussed for the Mathieu Fermi gas as a basis for generating a complete solution for the interacting neutron matter problem. As a starting point, we will consider a system of interacting neutrons in the absence of an external potential. Due to the homogeneity and isotropy of this system, we must find that the density $\rho(\mathbf{r}) = \rho_0$ and kinetic density $\tau(\mathbf{r}) = \tau_0$ are constants. Observing Eq. (3.26) we notice that in this scenario, the wavefunctions and eigenengergies of the neutrons will be analogous to the solutions of the FFG

problem, with z-axis Schrödinger equation:

$$-\frac{\hbar^2}{2m^*}\frac{\partial^2}{\partial z^2}\phi_{i,z}(z) + \left[U + \frac{\hbar^2}{2m^*}(k_x^2 + k_y^2)\right]\phi_{i,z}(z) = e_i\phi_{i,z}(z) \tag{3.62}$$

With the addition of an external potential, this Schrödinger equation is again modified to mirror the MFG Schrödinger equation:

$$-\frac{\hbar^2}{2m^*}\frac{\partial^2}{\partial z^2}\phi_{i,z}(z) + \left[U + \frac{\hbar^2}{2m^*}(k_x^2 + k_y^2) + 2v_q\cos(qz)\right]\phi_{i,z}(z) = e_i\phi_{i,z}(z) \tag{3.63}$$

The solutions to this equation are clearly Mathieu functions with well ordered eigenenergies as studied in Chapter 3; these will serve as an Ansatz to our iterative solution technique. For a system of N particles, we consider the set of the first N eigenpairs ordered by energy e_i, given by the solutions Eq. (2.22) and Eq. (2.23):

$$\Big\{\phi_i(\mathbf{r}), e_i(q)\Big\} \tag{3.64}$$

We use this set of wavefunctions to produce the neutron density and kinetic densities:

$$\rho(z) = \sum_i |\phi_i(\mathbf{r})|^2 \qquad , \qquad \tau(z) = \sum_i |\nabla\phi_i(\mathbf{r})|^2 \tag{3.65}$$

With the preliminary Ansatz in place, the general iterative solution scheme is as follows:

1. The finite difference solver is used to find the first N eigenstates and eigenenergies of the system:

   (a) A search space in the $n_x - n_y$ plane is established. The size of this search space is determined by the number of particles in the system and the strength of the external potential. For 4224 particles at a density

of 0.01 fm^{-3} and an external potential strength $v_q \leq 0.5E_F$, $n_x, n_y = 0, \pm 1, \ldots, \pm 11$ is sufficiently large enough such that no eigenstates and no eigenenergies will be omitted. This is the maximum search space required for any scenario that we will encounter in this research.

(b) It is important to note that since the tuples (n_x, n_y) only appear in Eq. (3.26) as $-n_x^2 - n_y^2$, this will introduce degeneracy into the eigenenergy solutions. These types of degeneracies are as follows:

i. $(0, 0)$

Is nondegenerate.

ii. $(\pm n_x, 0), (0, \pm n_y)$

Is fourfold degenerate where $n_x = n_y$.

iii. $(\pm n_x, \pm n_y), (\pm n_x, \mp n_y)$

Is fourfold degenerate if $n_x = n_y$.

Is eightfold degenerate if $n_x \neq n_y$.

Additionally, since the particles of interest are neutrons, all solutions will receive an additional factor of two to their degeneracies that corresponds to the +1/2 and -1/2 spin projections of the neutron. Taking these degeneracies into consideration, we can see that it is only needed to search in one eighth of the $n_x - n_y$ plane. For our research, this corresponds to $0 \leq n_x \leq n_y \leq 11$. We ascribe the appropriate degeneracy factor to the eigenenergy solutions based on the the corresponding (n_x, n_y) tuple.

(c) For each (n_x, n_y) in the search space, we are able to produce an ordered solution set for Eq. (3.26) using the finite difference method outlined in Section 3.2. The solution sets for every (n_x, n_y) will then be collated and

sorted by the eigenenergies of the states. The first N eigenstates will then be normalized.

2. With the sorted list of eigenpairs produced, we may then generate the density $\rho(\mathbf{r})$, kinetic density $\tau(\mathbf{r})$ and energy per particle E/N.

   (a) To produce the densitiy and kinetic density, we use the first N states including degeneracies to find:

$$\rho(z) = \sum_i \left|\phi_i(\mathbf{r})\right|^2 = \sum_i \left|\frac{1}{L}\exp\left[\frac{2i\pi}{L}(n_x x + n_y y)\right]\phi_{i,z}(z)\right|^2 = \frac{1}{L^2}\sum_i \left|\phi_{i,z}(z)\right|^2 \tag{3.66}$$

   and

$$\begin{aligned}\tau(z) &= \sum_i \left|\nabla\phi_i(\mathbf{r})\right|^2 = \sum_i \left|\nabla\left\{\frac{1}{L}\exp\left[\frac{2i\pi}{L}(n_x x + n_y y)\right]\phi_{i,z}(z)\right\}\right|^2 \\ &= \frac{1}{L^2}\sum_i \left|\exp\left[\frac{2i\pi}{L}(n_x x + n_y y)\right]\left(\frac{2i\pi}{L}n_x\phi_{i,z}(z), \frac{2i\pi}{L}n_y\phi_{i,z}(z), \frac{d}{dz}\phi_{i,z}(z)\right)\right|^2 \\ &= \frac{4\pi^2}{L^4}\sum_i \left[\left(n_x^2 + n_y^2\right)\phi_{i,z}^2(z) + \frac{L^2}{4\pi^2}\left(\frac{d}{dz}\phi_{i,z}(z)\right)^2\right]\end{aligned} \tag{3.67}$$

   (b) The energy per particle may then be obtained by substituting the above density and kinetic density into Eq. (3.2) and integrating over the volume. That is:

$$E/N = \int_V d\mathbf{r}\mathcal{H}(\mathbf{r}) \tag{3.68}$$

3. Steps 1 and 2 may then be repeated until the energy per particle has converged to within a specified tolerance or has reached a minimum, corresponding to the completion of the minimization procedure.

With the method complete, a wide range of initial conditions may be probed to examine the structure of the infinite neutron matter. In Fig. (3.2, 3.3, 3.4) we show the convergence of the density for set numbers of iterations for an average density of $\rho_0 = 0.01$ fm^{-3} and an external potential with $2v_q = 0.25E_F$ at 1 [Fig. (3.2)], 10 [Fig. (3.3)] and 40 [Fig. (3.4)] periods. The convergence for an average density of $\rho_0 = 0.01$ fm^{-3} and an external potential with $2v_q = 0.50E_F$ at 10 periods is illustrated in Fig. (3.5). Additionally we plot the convergences for an external potential with $2v_q = 0.25E_F$ at 10 periods for average densities of $\rho_0 = 0.05$ fm^{-3} Fig. (3.6) and $\rho_0 = 0.10$ fm^{-3} Fig. (3.7). We see that there is good convergence in relatively few iterations across all initial conditions.

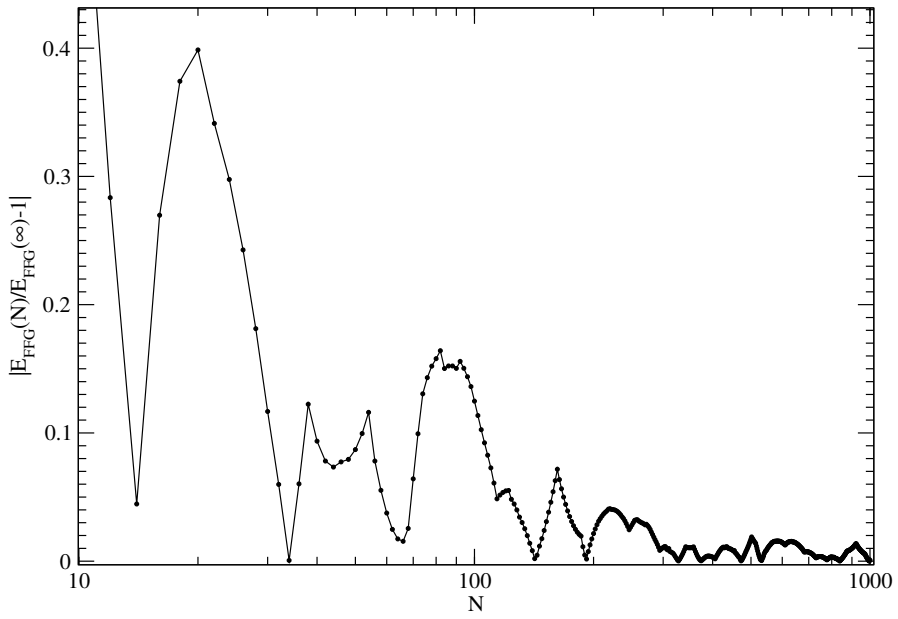

Figure 3.1: Relative error of N particle energy compared to TL energies shows magnitude of finite size effects. SLy4 parameterization at $\rho_0 = 0.01$fm^{-3}.

We can see in Fig. (3.1) that the energy per particle for varying particle numbers

using the SLy4 parameterization has a very similar form to that of the energy per particle in the free Fermi gas discussed in Chapter 2. However, we most importantly notice that the average relative error using the SLy4 parameterization is significantly higher for lower particle numbers. As we have previously discussed, the minimization of this error is the largest motivating factor to studying the case of 4224 particles.

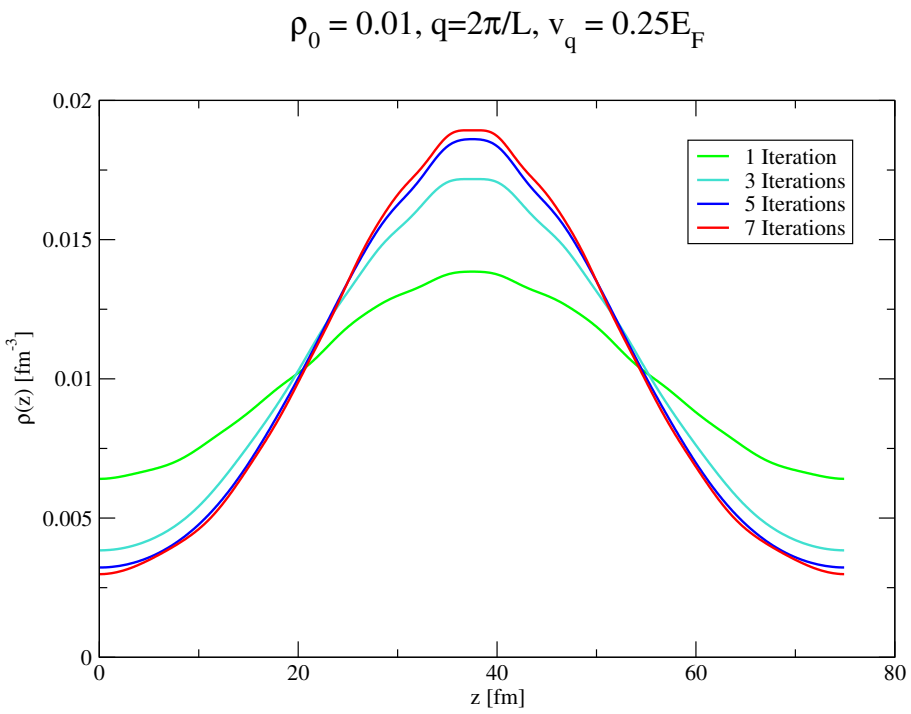

Figure 3.2: SLy4 $v_q = 0.25E_F$, 1 period potential at $\rho_0 = 0.01\text{fm}^{-3}$.

We may examine the behaviours of the densities through the use of the following equation that will later be derived in Chapter 4 describing the variation about the average density:

$$\delta\rho(q,z) = 2\cos(qz)\chi^{(1)}(q)v_q + \Big[\cos(qz) + 2\cos(3qz)\Big]\chi^{(3)}(q,q,-q)v_q^3 + \mathcal{O}(v_q^5) \quad (3.69)$$

As we will later see, the linear response term $\chi^{(1)}(q)$ acts as an amplitude gain tied to the periodicity of the external potential. We can see in Fig. (3.2, 3.3, 3.4) that for

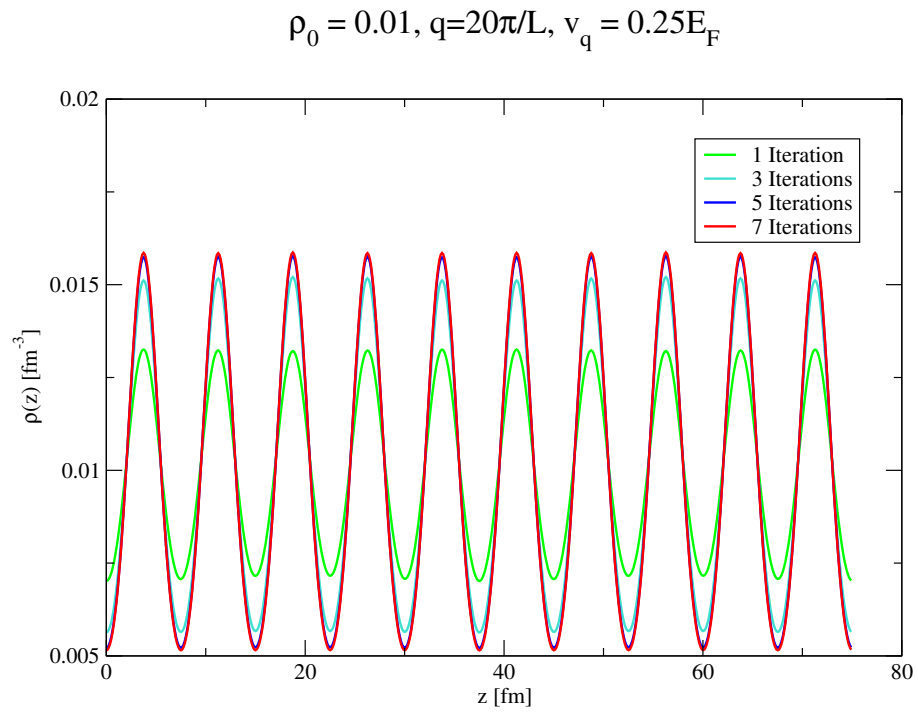

Figure 3.3: SLy4 $v_q = 0.25E_F$, 10 period potential at $\rho_0 = 0.01\text{fm}^{-3}$.

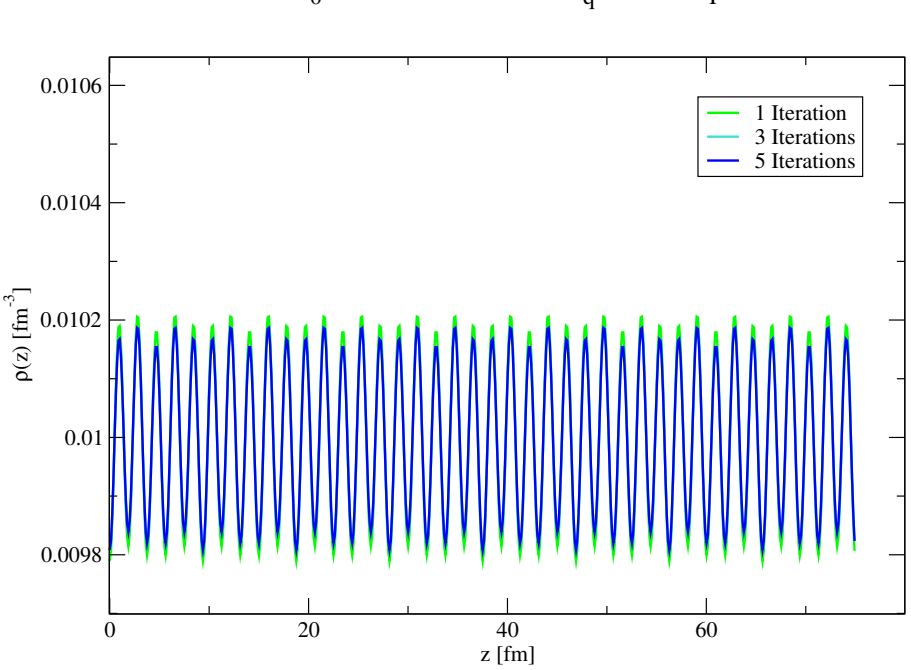

Figure 3.4: SLy4 $v_q = 0.25E_F$, 40 period potential at $\rho_0 = 0.01\text{fm}^{-3}$.

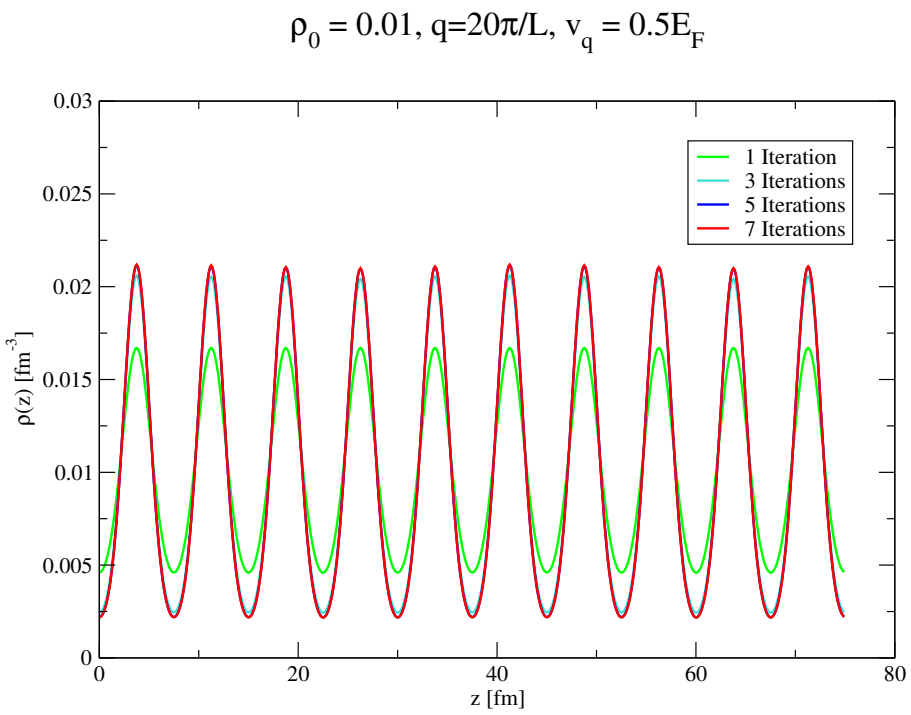

Figure 3.5: SLy4 $v_q = 0.5E_F$, 10 period potential at $\rho_0 = 0.01\text{fm}^{-3}$.

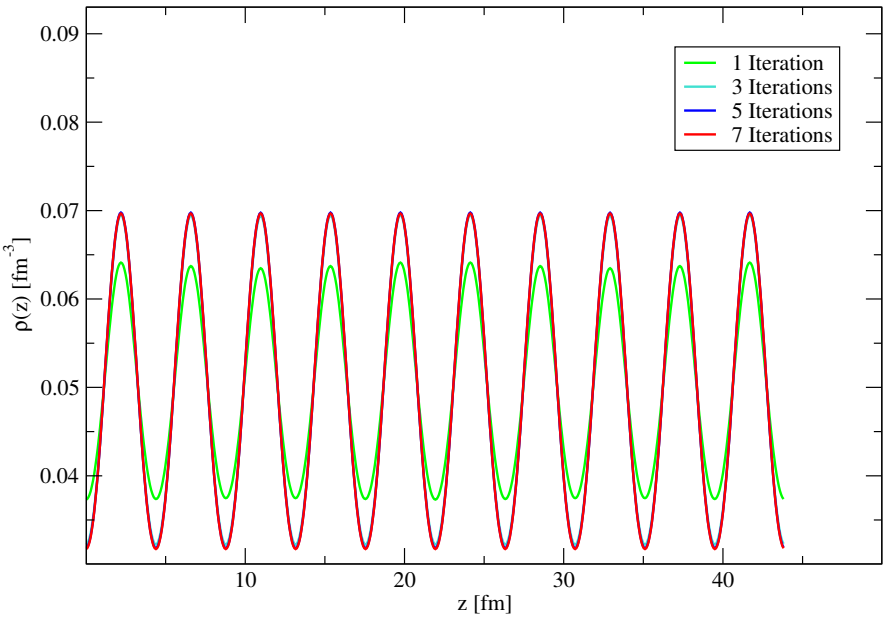

Figure 3.6: SLy4 $v_q = 0.25E_F$, 10 period potential at $\rho_0 = 0.05\text{fm}^{-3}$.

fixed v_q, with increasing q the amplitude of the density variations conversely decreases in accordance with the decrease in magnitude of the linear response functions $\chi^{(1)}(q)$ that are plotted in Chapter 4. Additionally, we can notice that while holding q fixed, increasing v_q has both the effect of increasing the amplitude of the variations and introducing higher order cosinusoidal terms that cause the density to deviate from a more regular sinusoidal form and can be most clearly seen in Fig. (3.5). We may finally notice in Fig. (3.6, 3.7) that the linear response terms $\chi^{(1)}(q)$ have implicit density dependencies where we can see that although both q and v_q are held fixed, the variations in density differ in the 0.05 fm^{-3} and 0.1 fm^{-3} density cases.

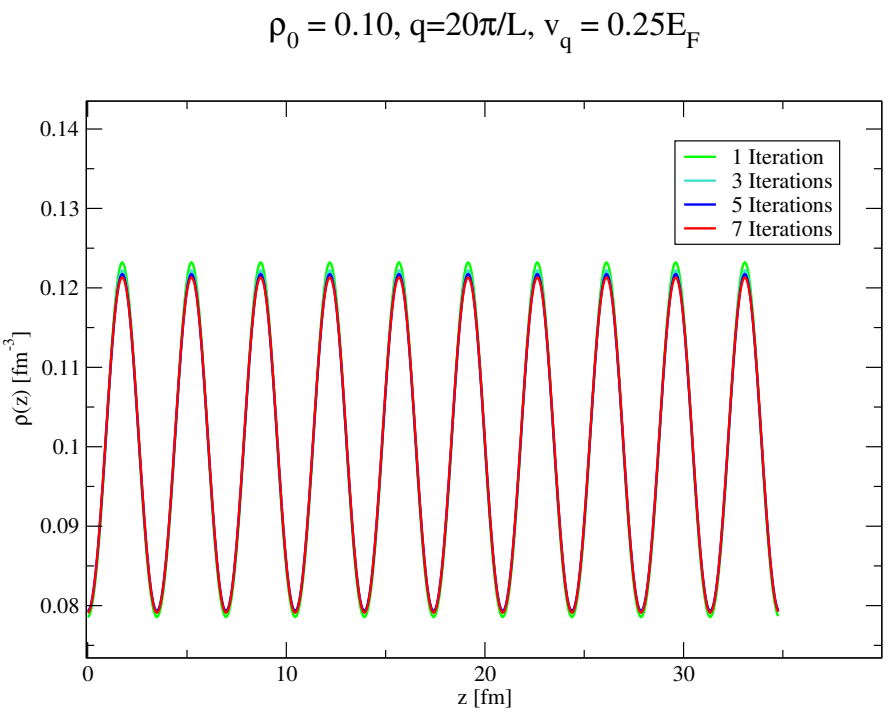

Figure 3.7: SLy4 $v_q = 0.25E_F$, 10 period potential at $\rho_0 = 0.10\text{fm}^{-3}$.

Chapter 4

Static Response

4.1 Static-Response Theory

We may use the Hartree-Fock solutions to find the linear response functions for neutron matter. We first consider the case of homogeneous and isotropic neutron matter in the absence of an external potential. This may be described by the Hamiltonian $\hat{H}_0$ with the ground state $\Psi_0(\mathbf{r})$, energy E_0 and density $\rho_0(\mathbf{r}) = |\Psi_0(\mathbf{r})|^2$. We must also note that the density $\rho_0(\mathbf{r}) = \rho_0$ is constant in accordance with homogeneity and isotropy. With the addition of a static external potential $v(\mathbf{r})$, the Hamiltonian for this perturbed system may now be written as:

$$\hat{H}_v = \hat{H}_0 + \int d\mathbf{r}\hat{\rho}(\mathbf{r})v(\mathbf{r}) \tag{4.1}$$

where effects due to $v(\mathbf{r})$ are coupled through one-body density operator $\hat{\rho}(\mathbf{r}) = \sum_{i=1}^{N} \delta(\mathbf{r} - \mathbf{r}_i)$. N is the number of particles in a finite volume V satisfying $N/V = \rho_0$ which is maintained in the thermodynamic limit ($V \to \infty, N \to \infty$). With these definitions in place, we see that the perturbed Hamiltonian is a functional of the external potential $v(\mathbf{r})$ and we may in turn write the ground state energy $E_v =$

$E_0[v]$ and density $\rho_v(\mathbf{r}) = \rho_0(\mathbf{r}, [v])$ as functionals of this potential. The functional expansion for the density $\rho_v(\mathbf{r})$ with respect to $v(\mathbf{r})$ is:

$$\begin{aligned}\rho_v(\mathbf{r}) &= \rho_0(\mathbf{r}, [0]) + \int d\mathbf{r}_1 \frac{\delta\rho_0(\mathbf{r}, [0])}{\delta v(\mathbf{r}_1)} v(\mathbf{r}_1) + \int d\mathbf{r}_1 d\mathbf{r}_2 \frac{\delta^2\rho_0(\mathbf{r}, [0])}{\delta v(\mathbf{r}_1)\delta v(\mathbf{r}_2)} v(\mathbf{r}_1)v(\mathbf{r}_2) + \cdots \\ &= \rho_0(\mathbf{r}, [0]) + \sum_{k=0}^{\infty} \frac{1}{k!} \int d\mathbf{r}_1 \cdots d\mathbf{r}_k \frac{\delta^k\rho_0(\mathbf{r}, [0])}{\delta v(\mathbf{r}_1) \cdots \delta v(\mathbf{r}_k)} v(\mathbf{r}_1) \cdots v(\mathbf{r}_k) \\ &= \rho_0 + \sum_{k=0}^{\infty} \frac{1}{k!} \int d\mathbf{r}_1 \cdots d\mathbf{r}_k \chi^{(k)}(\mathbf{r}_1 - \mathbf{r}, \ldots, \mathbf{r}_k - \mathbf{r}) v(\mathbf{r}_1) \cdots v(\mathbf{r}_k) \end{aligned} \tag{4.2}$$

where we note that $\rho_0(\mathbf{r}, [0]) = \rho_0$ is the unperturbed uniform density and the

$$\chi^{(k)}(\mathbf{r}_1 - \mathbf{r}, \ldots, \mathbf{r}_k - \mathbf{r}) = \frac{\delta^k\rho_0(\mathbf{r}, [0])}{\delta v(\mathbf{r}_1) \cdots \delta v(\mathbf{r}_k)} \tag{4.3}$$

terms are the density-density response functions. We would now like to write an analogous expression for the energy E_v using first order perturbation theory to derive the appropriate functional form. We first write the Hamiltonian in the form

$$\begin{aligned}\hat{H}_v &= \hat{H}_0 + \int d\mathbf{r} \hat{\rho}(\mathbf{r}) \lambda v(\mathbf{r}) = \hat{H}_0 + \int d\mathbf{r} \left(\sum_{i=1}^{N} \delta(\mathbf{r} - \mathbf{r}_i) \right) \lambda v(\mathbf{r}) \\ &= \hat{H}_0 + \lambda \sum_{i=1}^{N} v(\mathbf{r}_i) \end{aligned} \tag{4.4}$$

where $\lambda \in \mathbb{R}$ is a perturbative scaling factor to the external potential. To first order, perturbation theory dictates that we may write the perturbed wavefunction $\Psi_0(\mathbf{R}, [\lambda v])$ energy $E_0[\lambda v(\mathbf{r})]$ as:

$$\Psi_0(\mathbf{R}, [\lambda v]) = \Psi_0(\mathbf{R}, [0]) + \lambda \tilde{\Psi}_0(\mathbf{R}, [\lambda v]) + \mathcal{O}(\lambda^2) \tag{4.5}$$

and

$$E_0[\lambda v(\mathbf{r})] = E_0[0] + \lambda \int d\mathbf{R} \Psi_0^*(\mathbf{R}, [0]) \left(\sum_{i=1}^{N} v(\mathbf{r}_i) \right) \Psi_0(\mathbf{R}, [0]) + \mathcal{O}(\lambda^2) \tag{4.6}$$

Where $\Psi_0(\mathbf{R},[0])$ is the ground state wavefunction of the unperturbed Hamiltonian and $\tilde{\Psi}_0(\mathbf{R},[\lambda v])$ is the first order wavefunction perturbation. We have also employed the notation $\mathbf{R}=(\mathbf{r}_1,\ldots,\mathbf{r}_N)$ and $d\mathbf{R}=d\mathbf{r}_1\cdots d\mathbf{r}_N$. Substituting the expression:

$$\Psi_0(\mathbf{R},[0])=\Psi_0(\mathbf{R},[\lambda v])-\lambda\tilde{\Psi}_0(\mathbf{R},[\lambda v])+\mathcal{O}(\lambda^2) \tag{4.7}$$

into Eq (4.6) we find:

$$\begin{aligned}
E_0[\lambda v(\mathbf{r})] &= E_0[0]+\lambda\int d\mathbf{R}(\Psi_0^*(\mathbf{R},[\lambda v])-\lambda\tilde{\Psi}_0^*(\mathbf{R},[\lambda v])) \\
&\qquad\times\left(\sum_{i=1}^{N}v(\mathbf{r}_i)\right)(\Psi_0(\mathbf{R},[\lambda v])-\lambda\tilde{\Psi}_0(\mathbf{R},[\lambda v]))+\mathcal{O}(\lambda^2) \\
&= E_0[0]+\lambda\int d\mathbf{R}\Psi_0^*(\mathbf{R},[\lambda v])\left(\sum_{i=1}^{N}v(\mathbf{r}_i)\right)\Psi_0(\mathbf{R},[\lambda v])+\mathcal{O}(\lambda^2) \\
&= E_0[0]+\lambda\sum_{i=1}^{N}\int d\mathbf{R}v(\mathbf{r}_i)\Psi_0^*(\mathbf{R},[\lambda v])\Psi_0(\mathbf{R},[\lambda v])+\mathcal{O}(\lambda^2) \\
&= E_0[0]+\lambda\sum_{i=1}^{N}\int d\mathbf{R}v(\mathbf{r}_i)|\Psi_0(\mathbf{R},[\lambda v])|^2+\mathcal{O}(\lambda^2)
\end{aligned} \tag{4.8}$$

We can now note that

$$\begin{aligned}
\int d\mathbf{R}v(\mathbf{r}_i)|\Psi_0(\mathbf{R},[\lambda v])|^2 &= \int d\mathbf{r}_1,\ldots,d\mathbf{r}_N v(\mathbf{r}_i)|\Psi_0(\mathbf{R},[\lambda v])|^2 \\
&= \int d\mathbf{r}_i v(\mathbf{r}_i)\int d\mathbf{r}d\mathbf{r}_1,\ldots,d\mathbf{r}_{i-1},d\mathbf{r}_{i+1},\ldots,d\mathbf{r}_N|\Psi_0(\mathbf{R},[\lambda v])|^2
\end{aligned} \tag{4.9}$$

For Slater determinant wavefunctions $\Psi_0(\mathbf{R},[\lambda v])$ composed of single particle wavefunctions $\phi_k(\mathbf{r}_j,[\lambda v])$, we note that the normalized component terms:

$$\int d\mathbf{r}_j|\phi_k(\mathbf{r}_j,[\lambda v])|^2=1 \tag{4.10}$$

and the cross terms:

$$\int d\mathbf{r}_j \phi_k^*(\mathbf{r}_j, [\lambda v]) \phi_l(\mathbf{r}_j, [\lambda v]) = 0 \tag{4.11}$$

We can now recover

$$\int d\mathbf{r} d\mathbf{r}_1, \ldots, d\mathbf{r}_{i-1}, d\mathbf{r}_{i+1}, \ldots, d\mathbf{r}_N |\Psi_0(\mathbf{R}, [\lambda v])|^2 = \frac{1}{N} \sum_{k=1}^{N} |\phi_k(\mathbf{r}_i, [\lambda v])|^2 = \frac{1}{N} \rho_0(\mathbf{r}_i, [\lambda v]) \tag{4.12}$$

We can finally see that by substituting Eq. (4.12) into Eq. (4.9) and Eq. (4.9) into Eq. (4.8), we will recover

$$\begin{aligned} E_0[\lambda v(\mathbf{r})] &= E_0[0] + \lambda \sum_{i=1}^{N} \int d\mathbf{r}_i v(\mathbf{r}_i) \frac{1}{N} \rho_0(\mathbf{r}_i, [\lambda v]) + \mathcal{O}(\lambda^2) \\ &= E_0[0] + \lambda \int d\mathbf{r} v(\mathbf{r}) \rho_0(\mathbf{r}, [\lambda v]) \end{aligned} \tag{4.13}$$

where we have discarded all terms of $\mathcal{O}(\lambda^2)$ or smaller. We now substitute Eq. (4.2) into equation Eq. (4.13) and set $\lambda = 1$ to find:

$$\begin{aligned} E_0[\lambda v(\mathbf{r})] = E_0 + \rho_0 \int d\mathbf{r}_i v(\mathbf{r}_i) \\ + \sum_{k=0}^{\infty} \frac{1}{(k+1)!} \int d\mathbf{r} d\mathbf{r}_1 \cdots d\mathbf{r}_k \chi^{(k)}(\mathbf{r}_1 - \mathbf{r}, \ldots, \mathbf{r}_k - \mathbf{r}) v(\mathbf{r}) v(\mathbf{r}_1) \cdots v(\mathbf{r}_k) \end{aligned} \tag{4.14}$$

Decomposing the potential into its Fourier components $v_{\mathbf{q}}$, we find

$$v(\mathbf{r}) = \sum_{\mathbf{q}} v_{\mathbf{q}} \exp[i\mathbf{q} \cdot \mathbf{r}] \tag{4.15}$$

We can finally write the changes in density and energies as:

$$\delta\rho(\mathbf{r}) \equiv \rho_v(\mathbf{r}) - \rho_0 = \sum_{k=1}^{\infty} \frac{1}{k!} \sum_{\mathbf{q}_1,\ldots,\mathbf{q}_k} \chi^{(k)}(\mathbf{q}_1,\ldots,\mathbf{q}_k) v_{\mathbf{q}_1} \cdots v_{\mathbf{q}_k} \exp[i(\mathbf{q}_1 + \cdots + \mathbf{q}_k)\cdot\mathbf{r}] \tag{4.16}$$

and

$$\delta\varepsilon(\mathbf{r}) \equiv \frac{E_v}{N} - \frac{E_0}{N} = v_0 + \frac{1}{\rho_0} \sum_{k=1}^{\infty} \frac{1}{(k+1)!} \sum_{\mathbf{q}+\mathbf{q}_1+\cdots+\mathbf{q}_k=0} \chi^{(k)}(\mathbf{q}_1,\ldots,\mathbf{q}_k) v_{\mathbf{q}} v_{\mathbf{q}_1} \cdots v_{\mathbf{q}_k} \tag{4.17}$$

It is apparent that since the energy of the system must be independent of position, the exponential term $\exp[i(\mathbf{q}+\mathbf{q}_1+\cdots+\mathbf{q}_k)\cdot\mathbf{r}]$ that would normally appear in equation Eq. (4.17) must be 1 for all $\mathbf{r}$. This leads to the summation rule $\mathbf{q}+\mathbf{q}_1+\cdots+\mathbf{q}_k = 0$ that must be satisfied. We would now like to consider the case of a monochromatic potential of the form:

$$v(\mathbf{r}) = 2v_{\mathbf{q}}\cos(\mathbf{q}\cdot\mathbf{r}) = v_{\mathbf{q}}(\exp[i\mathbf{q}\cdot\mathbf{r}] + \exp[-i\mathbf{q}\cdot\mathbf{r}]) \tag{4.18}$$

The change in energy for this potential up to 4^{th} order in $v_{\mathbf{q}}$ is:

$$\begin{aligned}
\delta\varepsilon(\mathbf{q}) &= \frac{1}{2!\rho_0}\Big[\chi^{(1)}(\mathbf{q}) + \chi^{(1)}(-\mathbf{q})\Big] v_{\mathbf{q}}^2 \\
&+ \frac{1}{4!\rho_0}\Big[\chi^{(3)}(\mathbf{q},\mathbf{q},-\mathbf{q}) + \chi^{(3)}(\mathbf{q},-\mathbf{q},\mathbf{q}) + \chi^{(3)}(-\mathbf{q},\mathbf{q},\mathbf{q}) \\
&+ \chi^{(3)}(\mathbf{q},-\mathbf{q},-\mathbf{q}) + \chi^{(3)}(-\mathbf{q},\mathbf{q},-\mathbf{q}) + \chi^{(3)}(-\mathbf{q},-\mathbf{q},\mathbf{q})\Big] v_{\mathbf{q}}^4 + \mathcal{O}(v_{\mathbf{q}}^6) \\
&= \frac{1}{\rho_0}\chi^{(1)}(\mathbf{q}) v_{\mathbf{q}}^2 + \frac{1}{4\rho_0}\chi^{(3)}(\mathbf{q},\mathbf{q},-\mathbf{q}) v_{\mathbf{q}}^4 + \mathcal{O}(v_{\mathbf{q}}^6)
\end{aligned} \tag{4.19}$$

where all $\chi^{(1)}$ and $\chi^{(3)}$ terms are equivalent due to the homogeneity and isotropy conditions initially imposed. We note that this implies all terms of the form $\chi^{(2n)}$: $n \in \mathbb{Z}$ must be zero and $\delta\varepsilon(\mathbf{q})$ will be polynomial in only even powers of $v_{\mathbf{q}}$ for this

potential. Thus, with only $\chi^{(2n+1)} : n \in \mathbb{Z}$ terms nonzero, we may now write the change in density up to 3rd order in $v_{\mathbf{q}}$ as:

$$\begin{aligned}
\delta\rho(\mathbf{q},\mathbf{r}) &= \Big[\chi^{(1)}(\mathbf{q})\exp[i(\mathbf{q})\cdot\mathbf{r}] + \chi^{(1)}(-\mathbf{q})\exp[i(-\mathbf{q})\cdot\mathbf{r}]\Big]v_{\mathbf{q}} \\
&+ \frac{1}{3!}\Big[\chi^{(3)}(\mathbf{q},\mathbf{q},-\mathbf{q})\exp[i(\mathbf{q}+\mathbf{q}-\mathbf{q})\cdot\mathbf{r}] + \chi^{(3)}(\mathbf{q},-\mathbf{q},\mathbf{q})\exp[i(\mathbf{q}-\mathbf{q}+\mathbf{q})\cdot\mathbf{r}] \\
&+ \chi^{(3)}(-\mathbf{q},\mathbf{q},\mathbf{q})\exp[i(-\mathbf{q}+\mathbf{q}+\mathbf{q})\cdot\mathbf{r}] + \chi^{(3)}(\mathbf{q},-\mathbf{q},-\mathbf{q})\exp[i(\mathbf{q}-\mathbf{q}-\mathbf{q})\cdot\mathbf{r}] \\
&+ \chi^{(3)}(-\mathbf{q},\mathbf{q},-\mathbf{q})\exp[i(-\mathbf{q}+\mathbf{q}-\mathbf{q})\cdot\mathbf{r}] + \chi^{(3)}(-\mathbf{q},-\mathbf{q},\mathbf{q})\exp[i(-\mathbf{q}-\mathbf{q}+\mathbf{q})\cdot\mathbf{r}] \\
&+ \chi^{(3)}(\mathbf{q},\mathbf{q},\mathbf{q})\exp[i(\mathbf{q}+\mathbf{q}+\mathbf{q})\cdot\mathbf{r}] \\
&+ \chi^{(3)}(-\mathbf{q},-\mathbf{q},-\mathbf{q})\exp[i(-\mathbf{q}-\mathbf{q}-\mathbf{q})\cdot\mathbf{r}]\Big]v_{\mathbf{q}}^3 + \mathcal{O}(v_{\mathbf{q}}^5) \\
&= \Big[\exp[i(\mathbf{q})\cdot\mathbf{r}] + \exp[i(-\mathbf{q})\cdot\mathbf{r}]\Big]\chi^{(1)}(\mathbf{q})v_{\mathbf{q}} + \frac{1}{3!}\Big[3\exp[i(\mathbf{q})\cdot\mathbf{r}] + 3\exp[i(-\mathbf{q})\cdot\mathbf{r}] \\
&+ \exp[i(3\mathbf{q})\cdot\mathbf{r}] + \exp[i(-3\mathbf{q})\cdot\mathbf{r}]\Big]\chi^{(3)}(\mathbf{q},\mathbf{q},-\mathbf{q})v_{\mathbf{q}}^3 + \mathcal{O}(v_{\mathbf{q}}^5) \\
&= 2\cos(\mathbf{q}\cdot\mathbf{r})\chi^{(1)}(\mathbf{q})v_{\mathbf{q}} + \Big[\cos(\mathbf{q}\cdot\mathbf{r}) + 2\cos(3\mathbf{q}\cdot\mathbf{r})\Big]\chi^{(3)}(\mathbf{q},\mathbf{q},-\mathbf{q})v_{\mathbf{q}}^3 + \mathcal{O}(v_{\mathbf{q}}^5)
\end{aligned} \tag{4.20}$$

where we have again grouped the $\chi^{(1)}$ and $\chi^{(3)}$ terms. Thus, in the case of our chosen external potential along the z-axis, $v_q(\mathbf{r}) = 2v_q\cos(qz)$, we will recover:

$$\delta\varepsilon(q) = \frac{1}{\rho_0}\chi^{(1)}(q)v_q^2 + \frac{1}{4\rho_0}\chi^{(3)}(q,q,-q)v_q^4 + \mathcal{O}(v_q^6) \tag{4.21}$$

and

$$\delta\rho(q,z) = 2\cos(qz)\chi^{(1)}(q)v_q + \Big[\cos(qz) + 2\cos(3qz)\Big]\chi^{(3)}(q,q,-q)v_q^3 + \mathcal{O}(v_q^5) \tag{4.22}$$

For fixed values of $\mathbf{q}$ we calculate the energy per particle at various external potential strengths using the method outlined in Chapter 3 and use Eq. (4.21) to produce an even-ordered polynomial fit in powers of $v_{\mathbf{q}}$ to these points. We are interested in the leading order term of this fit, $\frac{1}{\rho_0}\chi^{(1)}(\mathbf{q})v_{\mathbf{q}}^2$, from which we may extract

the linear density-density response function $\chi^{(1)}(\mathbf{q})$. It is important to note that the fidelity of this fit is dependent on both the number of external potential strengths sampled as well as the order of the polynomial fit used, with fits of order higher than two producing better results in comparison to a simple quadratic fit. We have found that for the number of points used in our fits, a fourth order fit provides the best results while mitigating inaccuracies due to over-fitting. We can see that a fourth order fit consistently produces an accuracte fit across the entire range of conditions studied and is shown for external potentials with 1, 10 and 40 periods at densities of $\rho_0 = 0.01$ fm^{-3}, 0.05 fm^{-3} and 0.10 fm^{-3} in Fig. (4.1, 4.2, 4.3, 4.4, 4.5, 4.6, 4.7, 4.8, 4.9). We note that we use ε_{v_q} as the energy per particle at potential strength v_q. That is, $\varepsilon_{v_q} = \varepsilon(v_{\mathbf{q}})$.

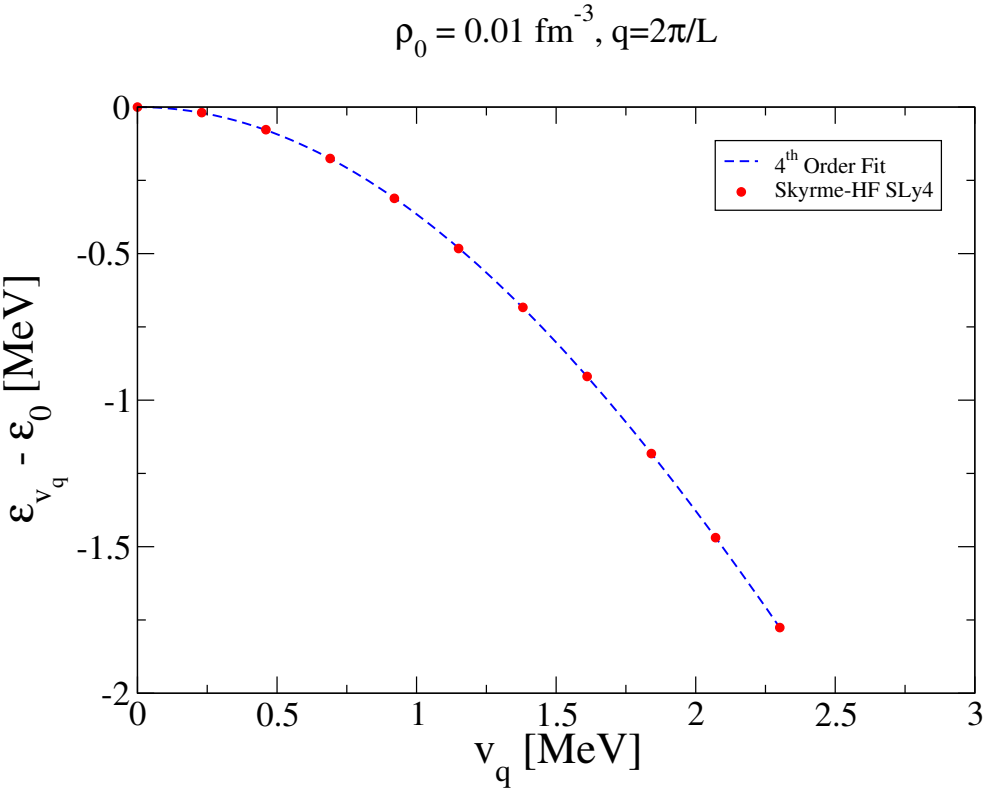

Figure 4.1: SLy4 4^{th} order fit, 1 period potential at $\rho_0 = 0.01\text{fm}^{-3}$.

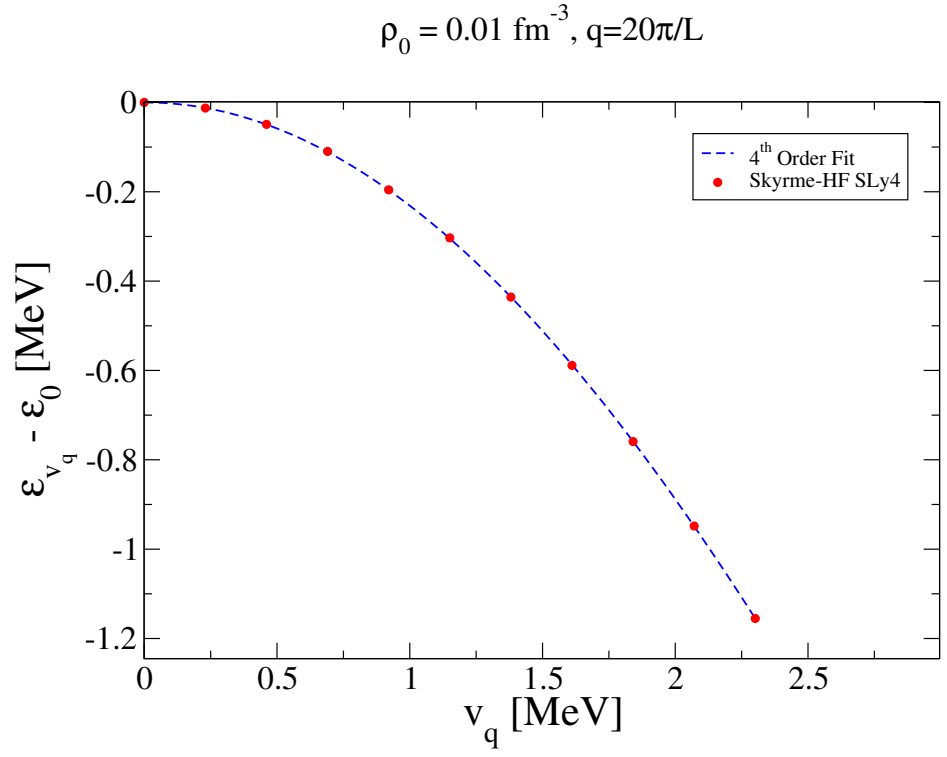

Figure 4.2: SLy4 4^{th} order fit, 10 period potential at $\rho_0 = 0.01\text{fm}^{-3}$.

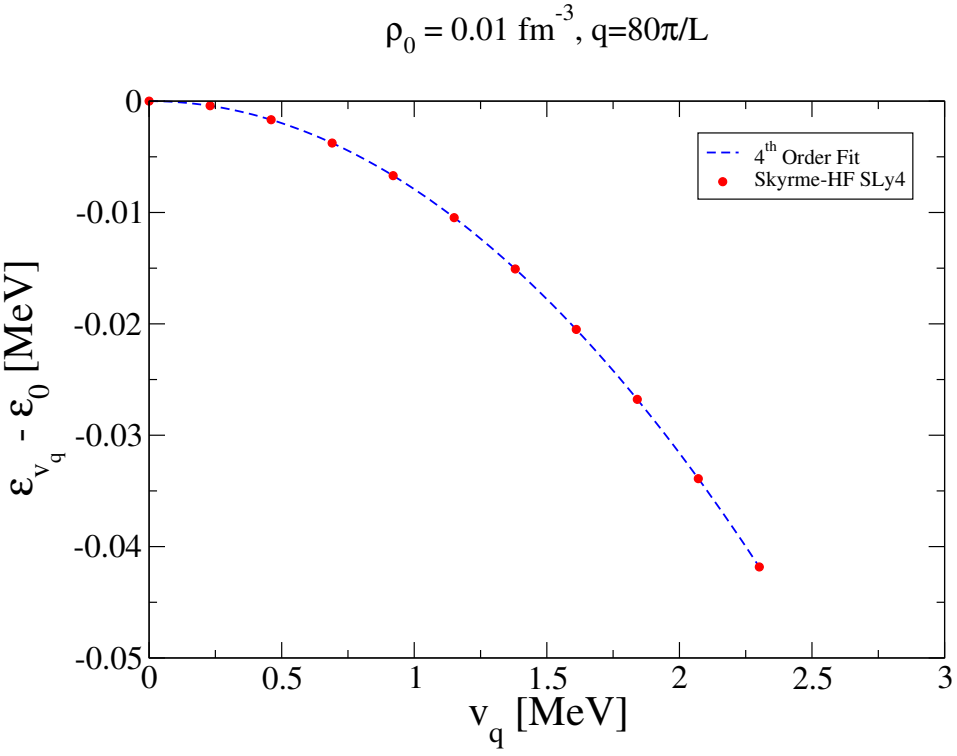

Figure 4.3: SLy4 4^{th} order fit, 40 period potential at $\rho_0 = 0.01\text{fm}^{-3}$.

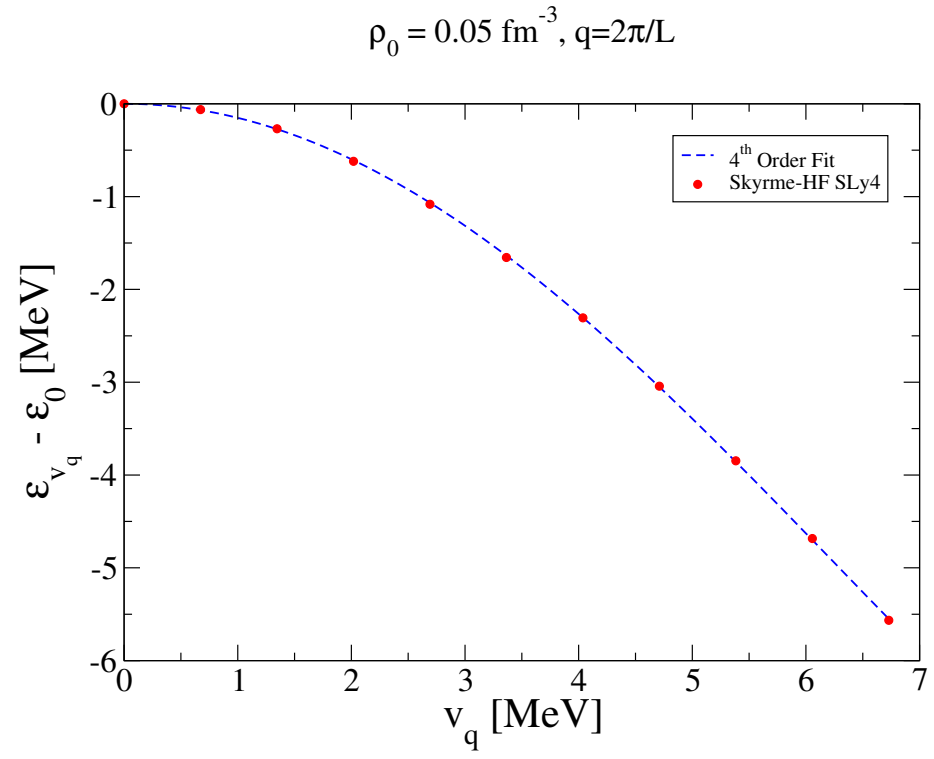

Figure 4.4: SLy4 4^{th} order fit, 1 period potential at $\rho_0 = 0.05\text{fm}^{-3}$.

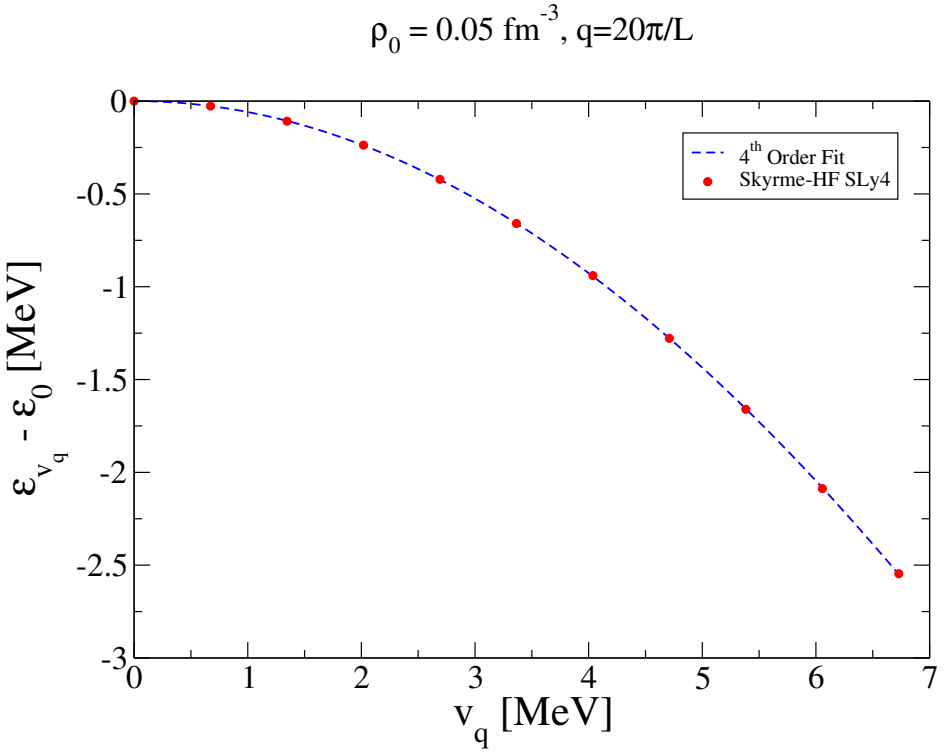

Figure 4.5: SLy4 4^{th} order fit, 10 period potential at $\rho_0 = 0.05\text{fm}^{-3}$.

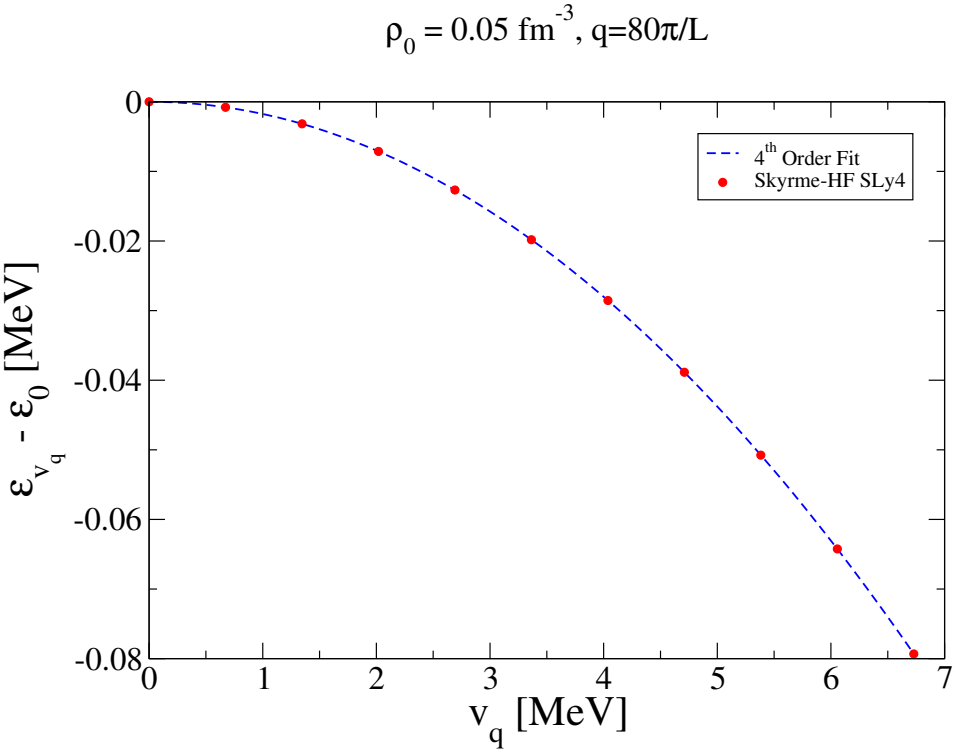

Figure 4.6: SLy4 4^{th} order fit, 40 period potential at $\rho_0 = 0.05\text{fm}^{-3}$.

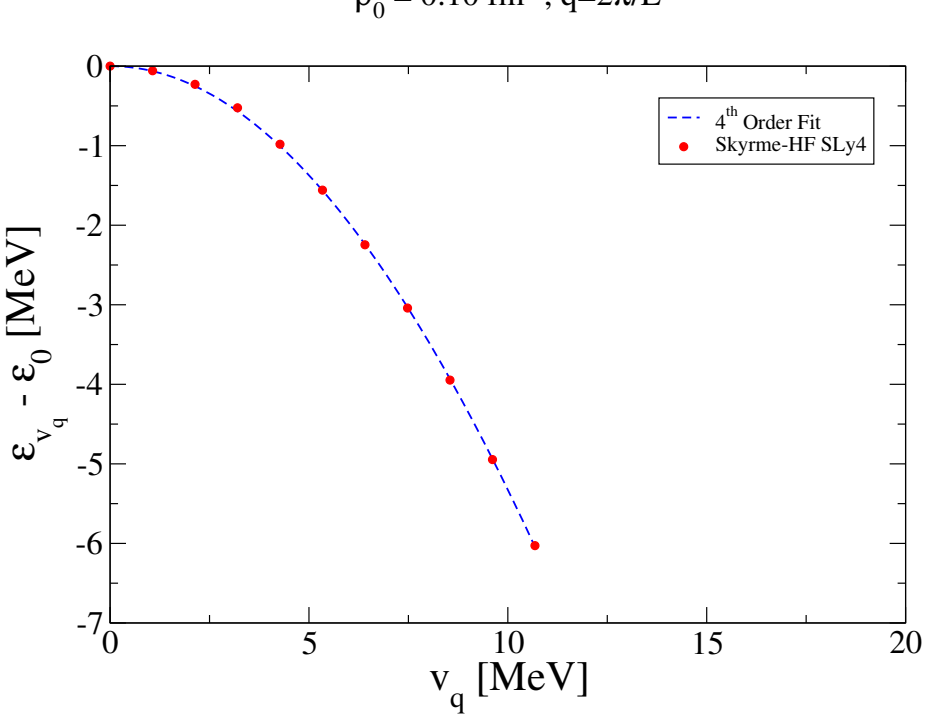

Figure 4.7: SLy4 4^{th} order fit, 1 period potential at $\rho_0 = 0.10\text{fm}^{-3}$.

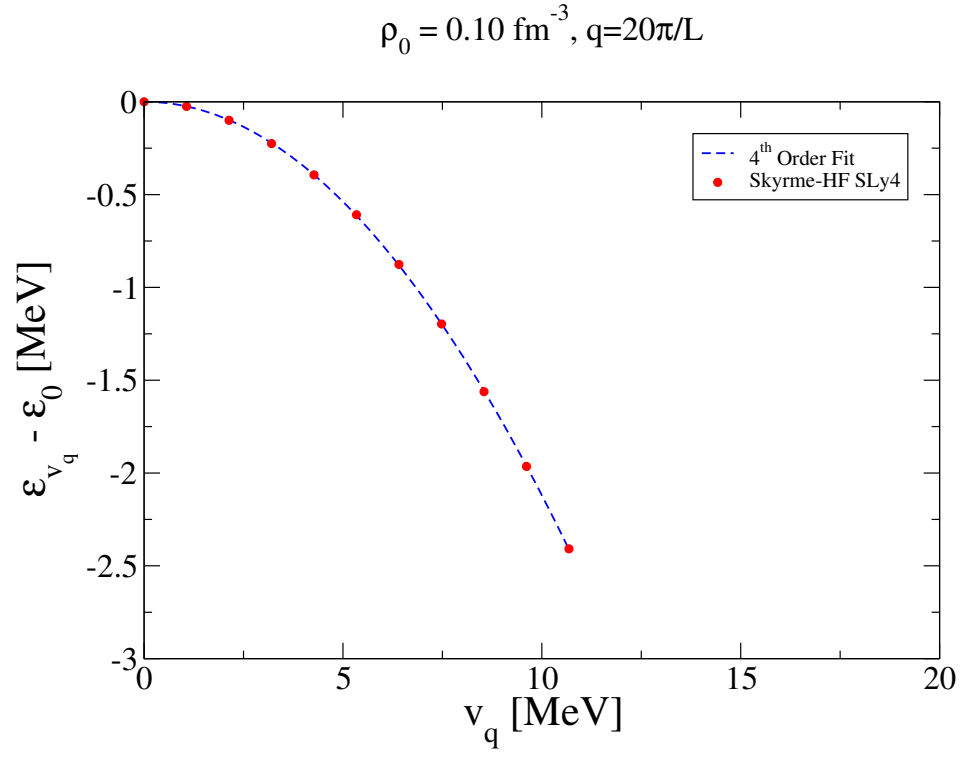

Figure 4.8: SLy4 4^{th} order fit, 10 period potential at $\rho_0 = 0.10\text{fm}^{-3}$.

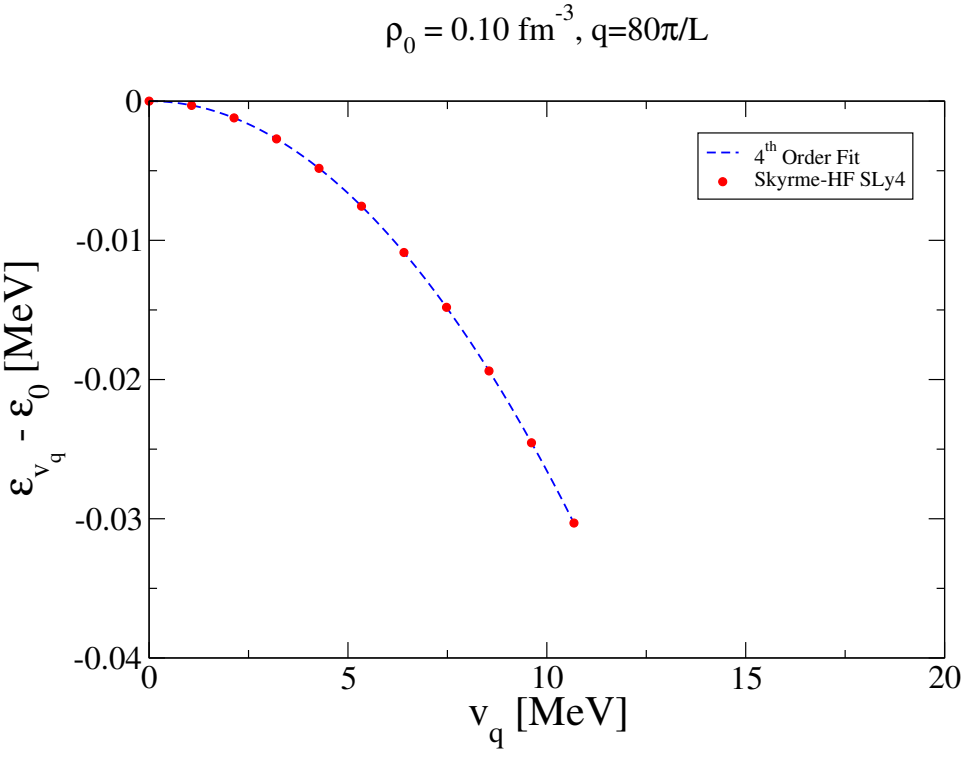

Figure 4.9: SLy4 4^{th} order fit, 40 period potential at $\rho_0 = 0.10\text{fm}^{-3}$.

4.2 Response Functions

Using the previous methods, we are able to calculate the linear density-density response function $\chi^{(1)}(q)$ at densities of 0.01fm^{-3}, 0.02fm^{-3}, 0.03fm^{-3}, 0.04fm^{-3}, 0.05fm^{-3}, 0.06fm^{-3}, 0.07fm^{-3}, 0.08fm^{-3}, 0.09fm^{-3}, 0.10fm^{-3} using the SLy4 parameterization of pure neutron matter. For our calculations we produced responses for cosinusoidal potentials with 1, 2, 3, 4, 6, 8, 10, 12, 16, 24, 32 and 40 periods fitting inside a box of length L containing 4224 particles. This is equivalent to the q values of 1, 2, 3, 4, 6, 8, 10, 12, 16, 24, 32 and 40 times $2\pi/L$.

Additionally, since we are unable to calculate $\chi(0)$ using these methods, we employ the compressibility sum rule where to first order:

$$\frac{1}{\chi(0)} = -\frac{\partial^2(\rho_0\varepsilon)}{\partial\rho_0^2} \approx -\frac{(\rho_0+\Delta\rho_0)\varepsilon(\rho_0+\Delta\rho_0) - 2\rho_0\varepsilon(\rho_0) + (\rho_0-\Delta\rho_0)\varepsilon(\rho_0-\Delta\rho_0)}{\Delta\rho_0^2} \tag{4.23}$$

Table 4.1: The $-\chi(0)/\rho_0$ response for densities ranging from 0.01 - 0.10 fm^{-3}

ρ_0	0.01 fm^{-3}	0.02 fm^{-3}	0.03 fm^{-3}	0.04 fm^{-3}	0.05 fm^{-3}
$-\chi(0)/\rho_0$	0.377 MeV^{-1}	0.300 MeV^{-1}	0.249 MeV^{-1}	0.202 MeV^{-1}	0.162 MeV^{-1}

ρ_0	0.06 fm^{-3}	0.07 fm^{-3}	0.08 fm^{-3}	0.09 fm^{-3}	0.10 fm^{-3}
$-\chi(0)/\rho_0$	0.129 MeV^{-1}	0.103 MeV^{-1}	0.083 MeV^{-1}	0.068 MeV^{-1}	0.056 MeV^{-1}

These identically match the analytically computable values, where we first note that $\varepsilon = \mathcal{H}$. In the absence of an external field, using $\tau_0 = \frac{3}{5}(3\pi^2)^{\frac{2}{3}}\rho_0^{\frac{5}{3}}$ we will find:

$$\begin{aligned}\mathcal{H} = &\frac{3\hbar^2}{10m}(3\pi^2)^{\frac{2}{3}}\rho_0^{\frac{5}{3}} + \frac{1}{4}t_0(1-x_0)\rho_0^2 + \frac{1}{24}t_3(1-x_3)\rho_0^{2+\sigma} \\ &+ \frac{3}{40}\big[(1-x_1)t_1 + 3(1+x_2)t_2\big](3\pi^2)^{\frac{2}{3}}\rho_0^{\frac{8}{3}}\end{aligned} \tag{4.24}$$

The analytic form of the compressibility sum rule gives:

$$
\begin{aligned}
-\chi(0)/\rho_0 &= \frac{1}{\rho_0}\left[\frac{\partial^2(\rho_0\mathcal{H})}{\partial\rho_0^2}\right] \\
&= \left[\frac{2\hbar^2}{3m}(3\pi^2)^{\frac{2}{3}}\rho_0^{\frac{2}{3}} + \frac{1}{2}t_0(1-x_0)\rho_0 + \frac{1}{24}t_3(1-x_3)(1+\sigma)(2+\sigma)\rho_0^{\sigma+1}\right. \\
&\quad \left. + \frac{1}{3}\big[(1-x_1)t_1 + 3(1+x_2)t_2\big](3\pi^2)^{\frac{2}{3}}\rho_0^{\frac{5}{3}}\right]^{-1} \qquad (4.25)
\end{aligned}
$$

Finally, examining the SLy4 linear density-density response functions shows that there is a very strong agreement with the analytic TL SLy response for all densities in the range 0.01 fm^{-3} to 0.10 fm $^{-3}$. The TL SLy4 response is given by the RPA response function $\chi^{(0,I)}_{RPA}$ as outlined in Appendix A. As expected, there are slight deviations from the TL RPA curve for small q/q_F as this region requires the largest sample of low lying momentum states that contribute to the general properties of the neutron matter. The Skyrme-Hartree-Fock responses for $q > 0$ are plotted as the red circles, the $q = 0$ responses are plotted as the green squares, and the TL SLy4 RPA responses are plotted as the blue dashed line in Fig. (4.10, 4.11, 4.12, 4.13, 4.14, 4.15, 4.16, 4.17, 4.18, 4.19).

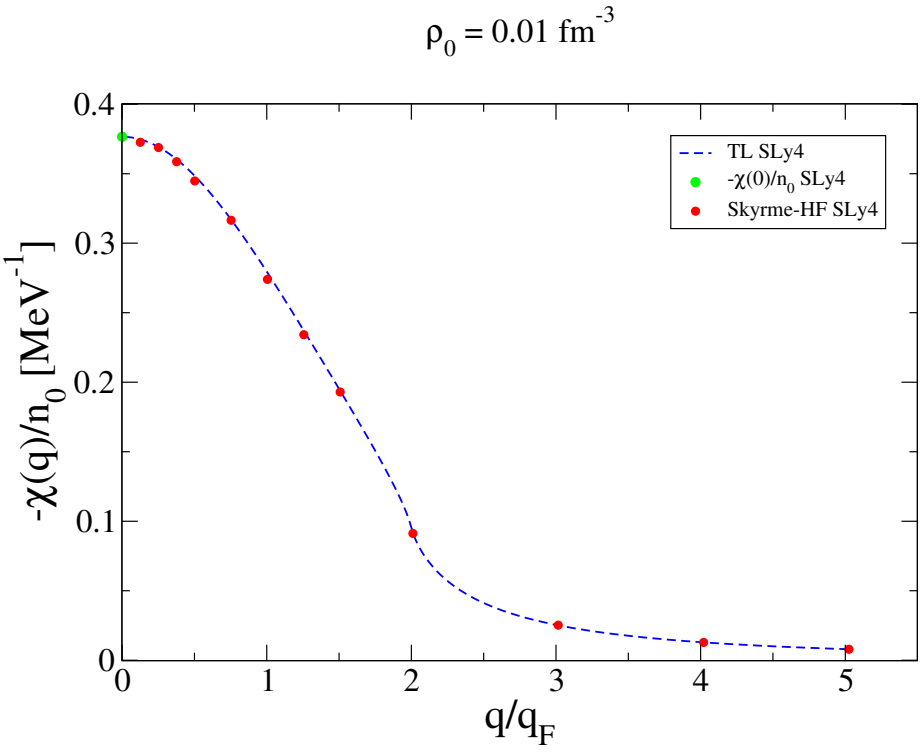

Figure 4.10: SLy4 linear density-density response for $\rho_0 = 0.01\text{fm}^{-3}$.

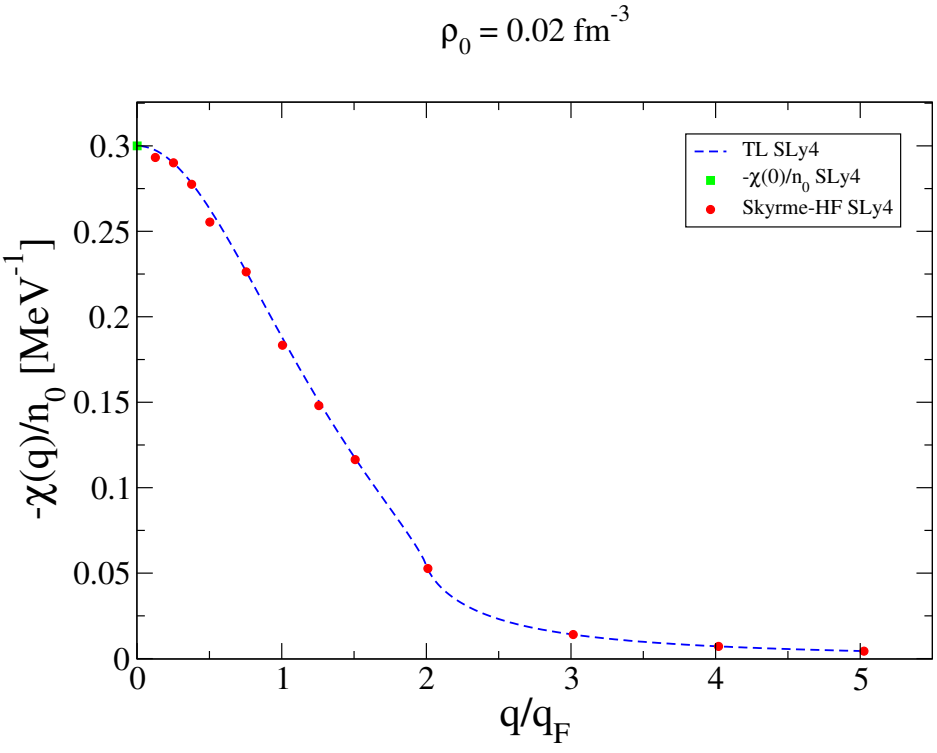

Figure 4.11: SLy4 linear density-density response for $\rho_0 = 0.02\text{fm}^{-3}$.

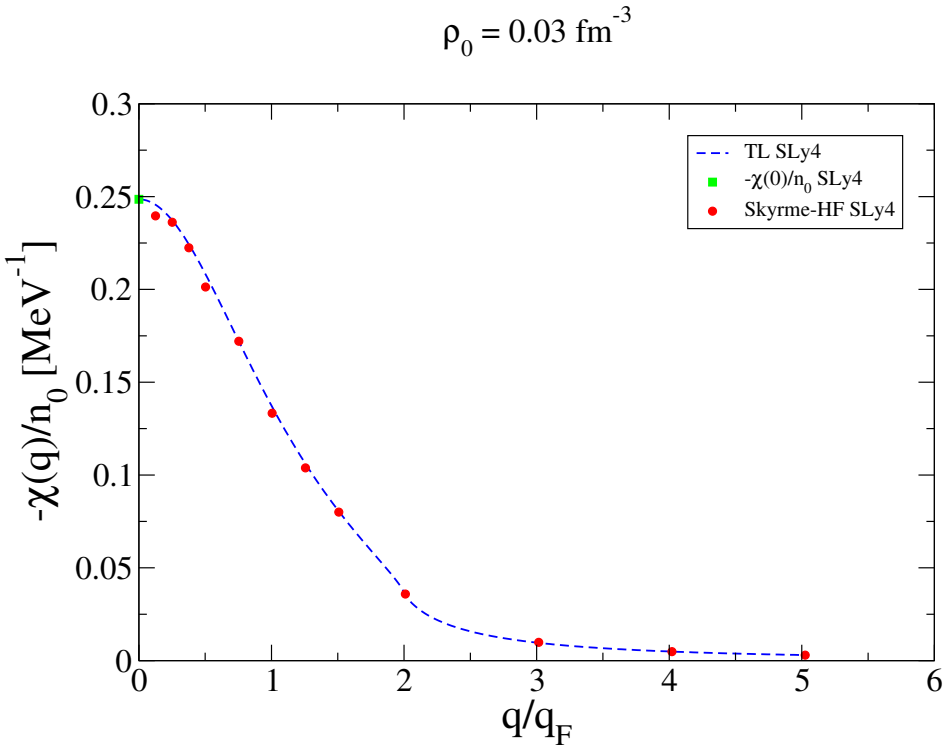

Figure 4.12: SLy4 linear density-density response for $\rho_0 = 0.03\text{fm}^{-3}$.

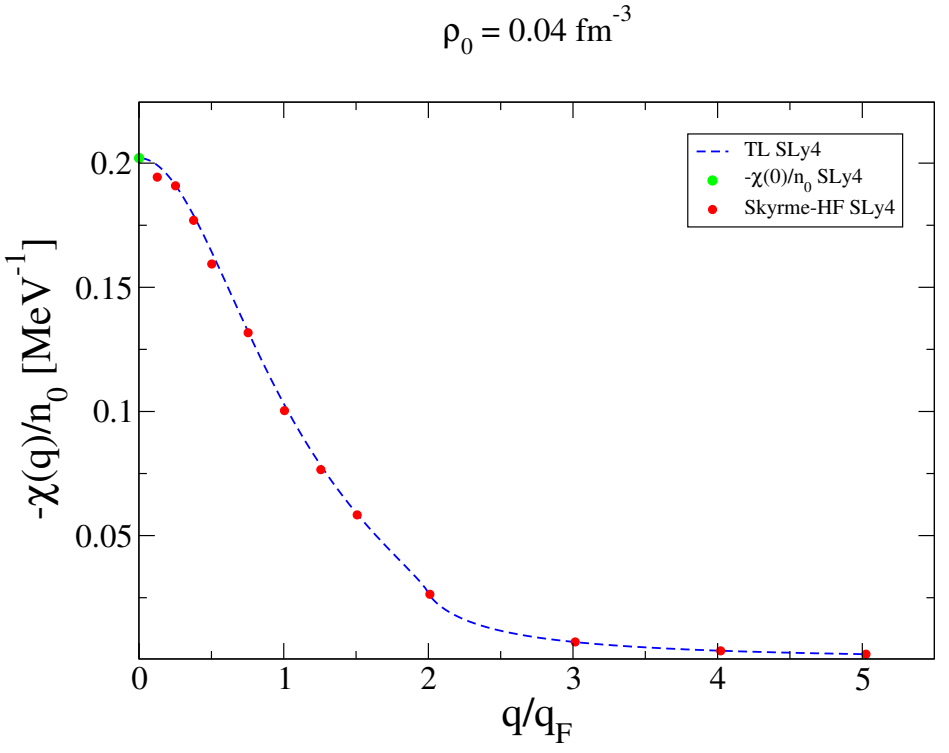

Figure 4.13: SLy4 linear density-density response for $\rho_0 = 0.03\text{fm}^{-3}$.

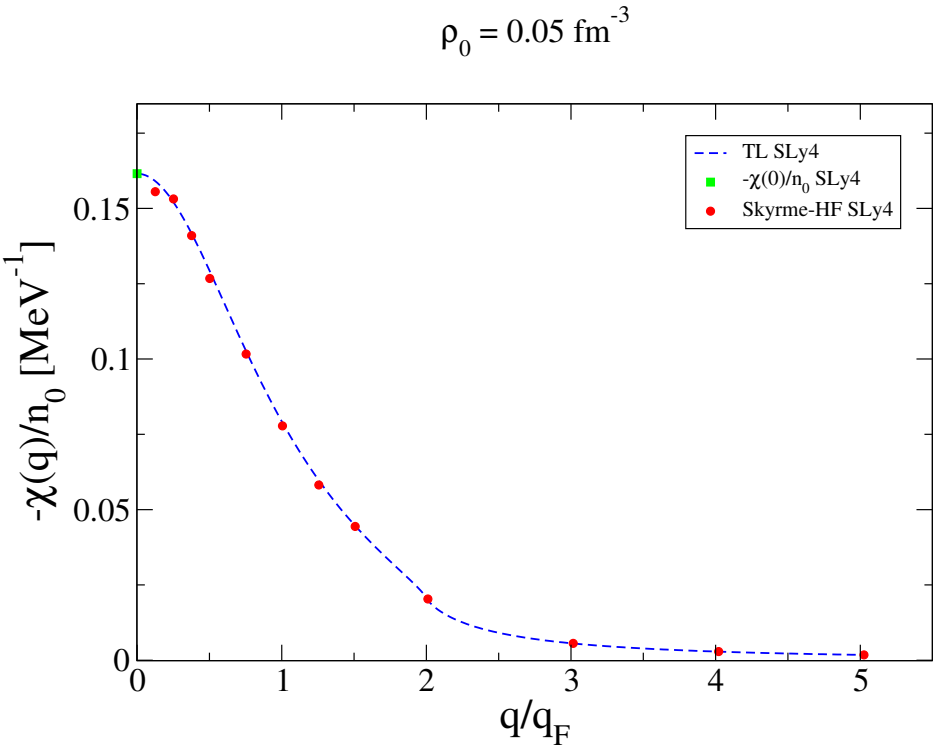

Figure 4.14: SLy4 linear density-density response for $\rho_0 = 0.05\text{fm}^{-3}$.

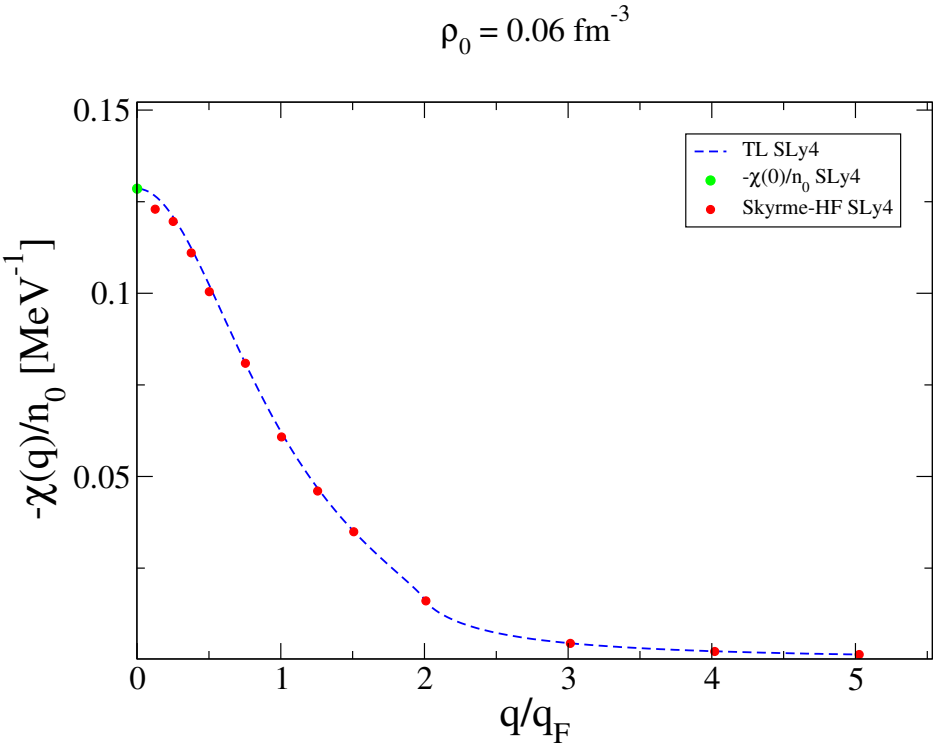

Figure 4.15: SLy4 linear density-density response for $\rho_0 = 0.06\text{fm}^{-3}$.

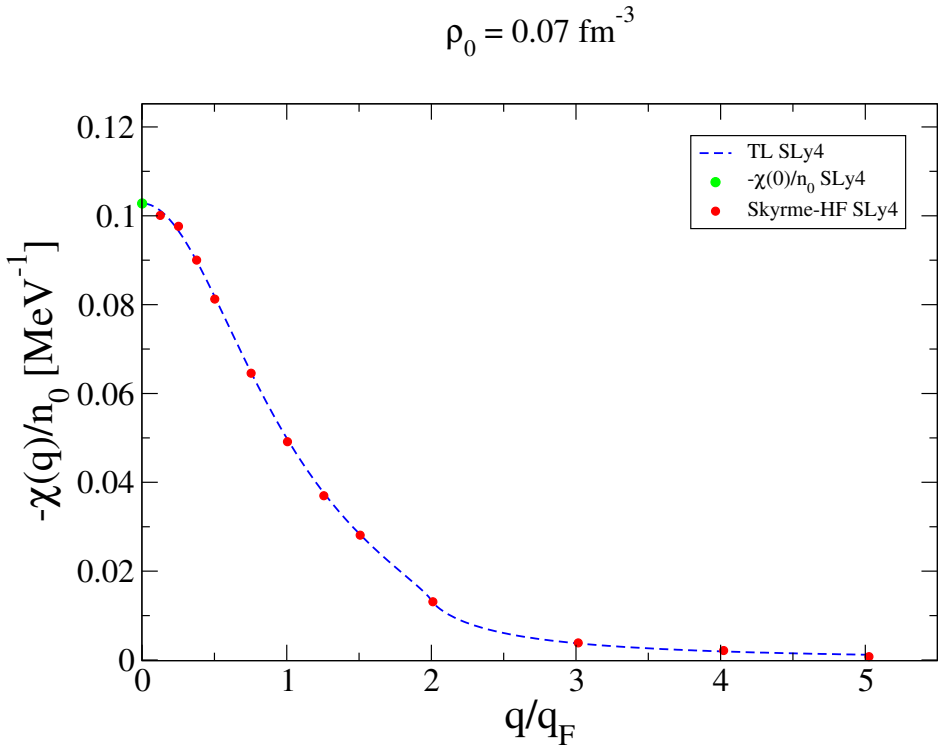

Figure 4.16: SLy4 linear density-density response for $\rho_0 = 0.07\text{fm}^{-3}$.

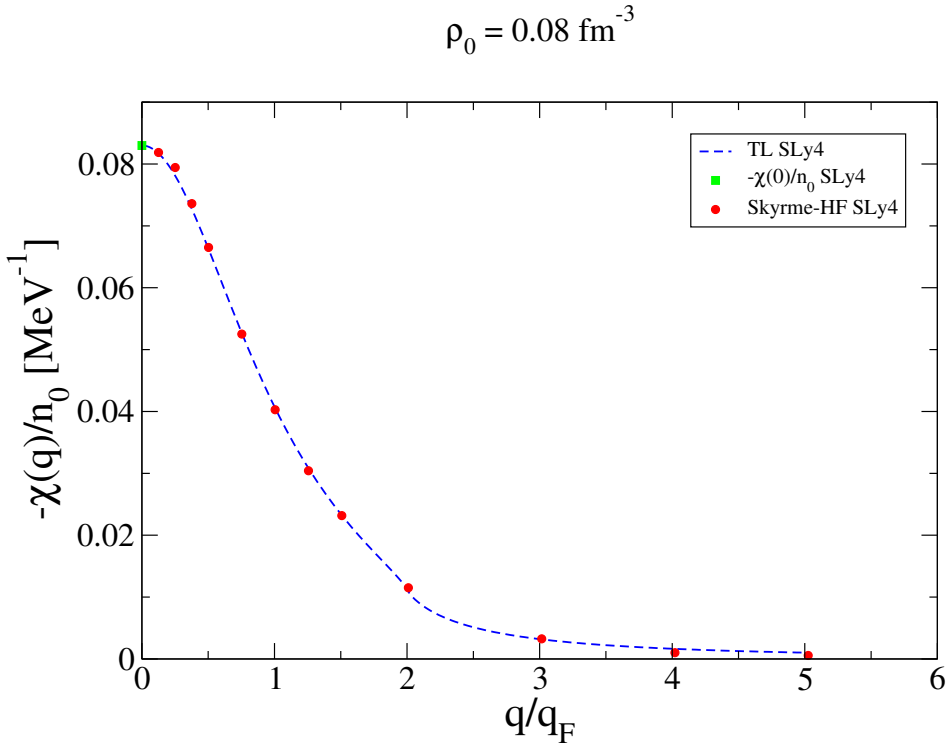

Figure 4.17: SLy4 linear density-density response for $\rho_0 = 0.08\text{fm}^{-3}$.

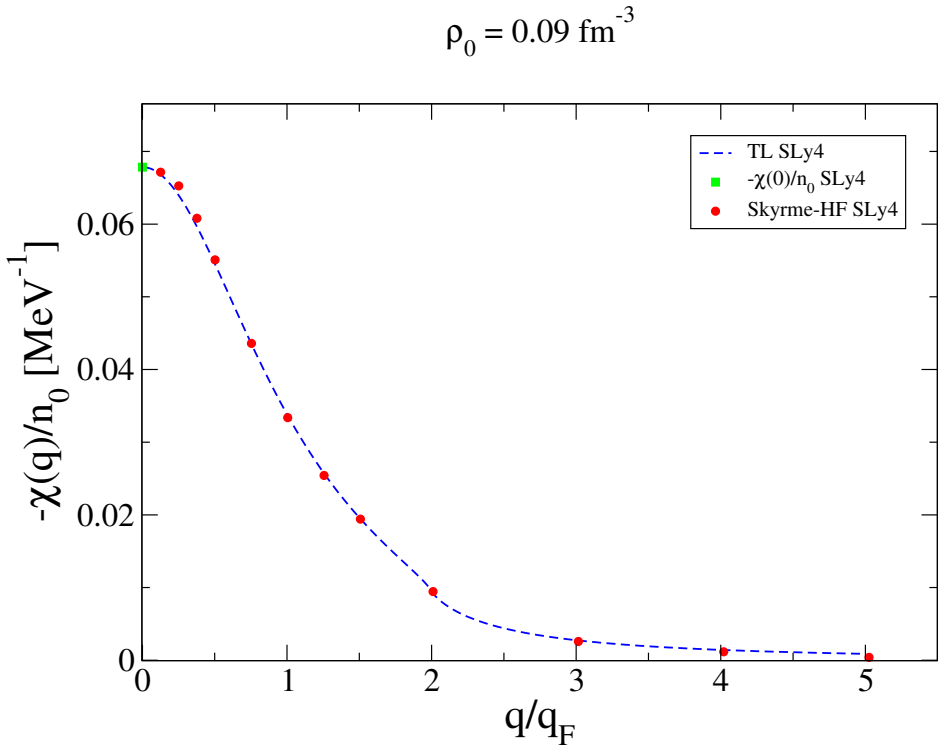

Figure 4.18: SLy4 linear density-density response for $\rho_0 = 0.09\text{fm}^{-3}$.

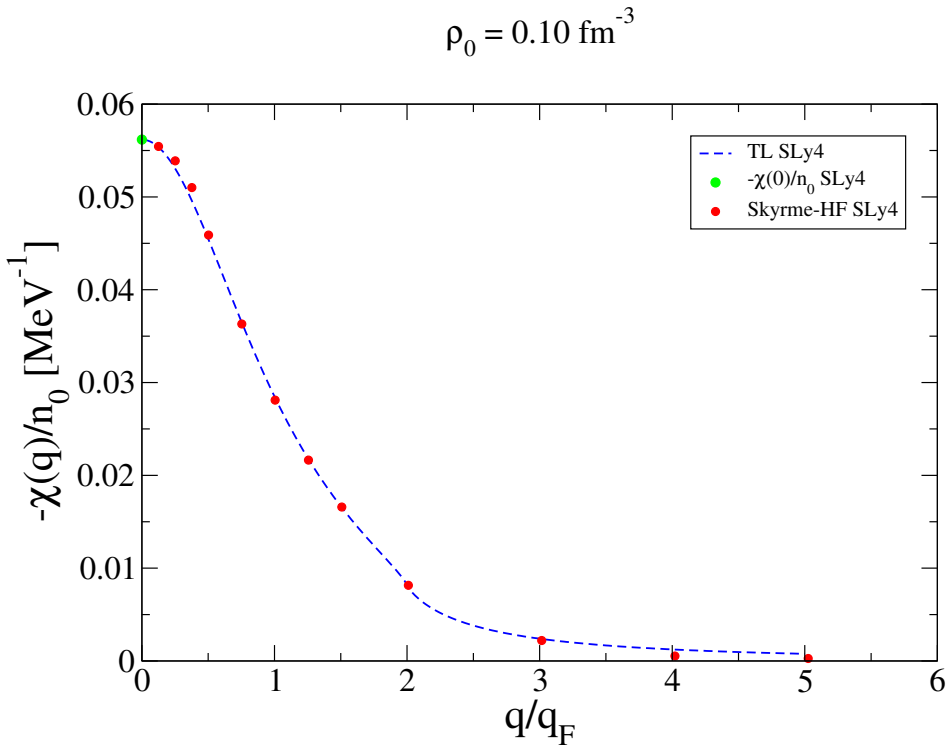

Figure 4.19: SLy4 linear density-density response for $\rho_0 = 0.10\text{fm}^{-3}$.

Chapter 5

Summary & Conclusion

Concluding, we examined how infinite neutron matter behaves in the presence of a periodic external field, employing Hartree-Fock methods coupled with energy density functional theory. We constructed a toy model of the complete system by modeling neutron matter first as a non-interacting free Fermi gas and examining the effects the addition of an external potential. This provided insight into multiple areas of our studies. We were first able to understand the size of system needed to be able to minimize finite size effects. In contrast to traditional Monte Carlo simulations that use 66 particle systems, we found that the Hartree-Fock methods used allowed for a significantly larger system of 4224 particles to be studied due to the reduction in compuational resources needed; greatly reducing finite size effect contributions. We also learned about how the bifurcation of energy levels as a result of the addition of the external potential allowed for a greater understanding of the single particle states used due to the reduction in degeneracy.

Finally, we were able to compute the linear density-density static response functions. These showed very good agreement with analytic results over both a wide range of densities and at high and low periodicities of the external potential. As

such, the Skyrme-Hartree-Fock method cements itself as an extremely robust technique for modeling the infinite neutron matter system, while also providing insights into its structure not achieved through analytic methods.

Appendix A

The RPA response function

For pure neutron matter in the $S = 0$ channel the linear density-density response function is given by the RPA response $\chi^{(0,I)}_{RPA}$ [13, 14]:

$$\begin{aligned}\frac{\chi_{HF}}{\chi^{(0,I)}_{RPA}} &= 1 - \tilde{W}^{(0,I)}_1\chi_0 + \frac{1}{2}q^2W^{(0,I)}_3\chi_0 + W^{(0,I)}_2\Big(\frac{q^2}{2}\chi_0 - 2k_F^2\chi_2\Big) \\ &+ [W^{(0,I)}_2]^2k_F^4\Big(- \chi_0\chi_4 + \chi_2^2 + \frac{m^{*2}\omega^2}{k_F^4\hbar^4}\chi_0^2 - \frac{m^*q^2}{6\pi^2k_F\hbar^2}\chi_0\Big) \\ &+ \frac{2m^{*2}\omega^2}{q^2\hbar^4}\frac{W^{(0,I)}_2 - W^{(0,I)}_3}{1 - \frac{2m^{*2}k_F^3}{3\pi^2\hbar^4}(W^{(0,I)}_2 - W^{(0,I)}_3)}\chi_0 \end{aligned} \tag{1}$$

where

$$\tilde{W}^{(0,I)}_1 = W^{(0,I)}_1(q) + \frac{q^4[W^{(I)}_{SO}]^2(\beta_2 - \beta_3)}{1 + q^2(\beta_2 - \beta_3)[W^{(1,I)}_2 - W^{(1,I)}_3 - \frac{1}{2}W^{(I)}_{T1}]} \tag{2}$$

We note that in our original calculations we have not included effects due to spin-orbit and tensor interactions. This must mean that both $W^{(I)}_{SO} = W^{(I)}_{T1} = 0$, hence:

$$\tilde{W}^{(0,I)}_1 = W^{(0,I)}_1(q) \tag{3}$$

Additionally, in pure neutron matter we also find that [27]:

$$W^{(\alpha)}_3 = 0 \tag{4}$$

In the case of a static response, we will also note that we do not consider the time evolution of the system, thus $\omega = 0$ and our response is reduced to:

$$\begin{aligned}\frac{\chi_{HF}}{\chi^{(0,I)}_{RPA}} &= 1 - W_1^{(0,I)}\chi_0 + W_2^{(0,I)}\Big(\frac{q^2}{2}\chi_0 - 2k_F^2\chi_2\Big) \\ &\quad + [W_2^{(0,I)}]^2 k_F^4\Big(- \chi_0\chi_4 + \chi_2^2 - \frac{m^* q^2}{6\pi^2 k_F \hbar^2}\chi_0\Big)\end{aligned} \tag{5}$$

The constants $W_i^{(\alpha)}$ for pure neutron matter are tabulated below [15]:

(α)	$W_1^{(\alpha)}/2$	$W_2^{(\alpha)}/2$
$(0,n)$	$2\big(C_0^{\rho,0} + C_1^{\rho,0}\big) + (2+\gamma)(1+\gamma)\big[C_0^{\rho\gamma} + C_1^{\rho\gamma}\big]\rho^\gamma$ $-q^2\big[2C_0^{\Delta\rho} + 2C_1^{\Delta\rho} + \frac{1}{2}2C_0^{\tau} + \frac{1}{2}2C_1^{\tau}\big]$	$C_0^\tau + C_1^\tau$
$(1,n)$	$2\big(C_0^{s,0} + C_1^{s,0} + C_0^{s\gamma} + C_1^{s\gamma}\rho^\gamma\big)$ $-q^2\big[2C_0^{\Delta s} + 2C_1^{\Delta s} + \frac{1}{2}C_0^{T} + \frac{1}{2}C_1^{T}\big]$	$C_0^T + C_1^T$

(6)

These coupling constants, C, are tabulated below in terms of the Skyrme interaction parameters:

$$\begin{aligned}C_0^{\Delta\rho} &= \frac{3}{192}(-9t_1 + 5t_2 + 4t_2x_2) \\ C_0^{\tau} &= \frac{12}{192}(3t_1 5t_2 + 4t_2x_2) \\ C_1^{\Delta\rho} &= \frac{3}{192}(3t_1 + 6t_1x_1 + t_2 + 2t_2x_2) \\ C_1^{\tau} &= \frac{12}{192}(-t_1 - 2t_1x_1 + t_2 + 2t_2x_2)\end{aligned} \tag{7}$$

As well as the definitions

$$C_0^\rho[\rho_0] = \frac{3}{8}t_0 + \frac{3}{48}t_3\rho_0^\alpha \tag{8}$$

$$C_1^\rho[\rho_0] = -\frac{1}{8}t_0(2x_0+1) - \frac{1}{48}t_3(2x_3+1)\rho_0^\alpha \tag{9}$$

We also write the generalized Lindhard functions $\chi_{2i}(\nu,k)$: $i=0,1,2$, in terms of the dimensionless variables $k=q/2k_F$ and $\nu=\omega m^*/qk_F$ [27].

$$\chi_0(\nu,k)=-\frac{m^*k_F}{4\pi^2\hbar^2}\Big[1+A_+(\nu,k)+A_-(\nu,k)\Big] \tag{10}$$

$$\chi_2(\nu,k)=-\frac{m^*k_F}{8\pi^2\hbar^2}\Big[3+k^2-\nu^2+(1+(k-\nu)^2)A_+(\nu,k)+(1+(k+\nu)^2)A_-(\nu,k)\Big] \tag{11}$$

$$\begin{aligned}\chi_4(\nu,k)=-\frac{m^*k_F}{12\pi^2\hbar^2}\Big[&5+\frac{49}{3}k^2+k^4-\nu^2+16k^2\nu^2-\nu^4\\&+(1+k^2+k^4-4k\nu-2k^3\nu+\nu^2+18k^2\nu^2-2k\nu^3+\nu^4)A_+(\nu,k)\\&+(1+k^2+k^4+4k\nu+2k^3\nu+\nu^2+18k^2\nu^2+2k\nu^3+\nu^4)A_-(\nu,k)\Big]\end{aligned} \tag{12}$$

where

$$A_\pm(\nu,k)=\frac{1}{4k}[1-(k\pm\nu)^2]\Big(\log\Big|\frac{k\pm\nu+1}{k\pm\nu-1}\Big|\mp i\pi\mathrm{sign}(\nu)\theta(1-(k\pm\nu)^2)\Big) \tag{13}$$

We can now note that in the case of a static response, both $\omega=0$ and $\nu=0$ allowing us to recover the expressions:

$$\chi_0(0,k)=-\frac{m^*k_F}{4\pi^2\hbar^2}\Big[1+A_+(0,k)+A_-(0,k)\Big] \tag{14}$$

$$\chi_2(0,k)=-\frac{m^*k_F}{8\pi^2\hbar^2}\Big[3+k^2+(1+k^2)(A_+(0,k)+A_-(0,k))\Big] \tag{15}$$

$$\chi_4(0,k)=-\frac{m^*k_F}{12\pi^2\hbar^2}\Big[5+\frac{49}{3}k^2+k^4+(1+k^2+k^4)(A_+(0,k)+A_-(0,k))\Big] \tag{16}$$

Simplifying, we note that:

$$A_+(0,k) + A_-(0,k) = \frac{1}{4k}[1-k^2]\Big(2\log\Big|\frac{k+1}{k-1}\Big| + i\pi\text{sign}(0)\theta(1-k^2) - i\pi\text{sign}(0)\theta(1-k^2)\Big)$$
$$= \frac{1}{2k}[1-k^2]\log\Big|\frac{k+1}{k-1}\Big| \tag{17}$$

Bibliography

[1] James M. Lattimer and F. Douglas Swesty. A generalized equation of state for hot, dense matter. *Nuclear Physics A*, 535(2):331–376, December 1991.

[2] James M. Lattimer. The nuclear equation of state and neutron star masses. *Annual Review of Nuclear and Particle Science*, 62(1):485–515, November 2012.

[3] J. M. Lattimer and M. Prakash. Neutron star structure and the equation of state. *The Astrophysical Journal*, 550(1):426–442, March 2001.

[4] M. Akbari-Moghanjoughi. Generalized charge-screening in relativistic Thomas–Fermi model. *Physics of Plasmas*, 21(10):102702, October 2014.

[5] J. R. Oppenheimer and G. M. Volkoff. On massive neutron cores. *Physical Review*, 55(4):374–381, February 1939.

[6] C. J. Yang, M. Grasso, and D. Lacroix. From dilute matter to the equilibrium point in the energy-density-functional theory. *Physical Review C*, 94(3):031301, September 2016.

[7] 89(1):015007, March 2017.

[8] Aurel Bulgac, Michael McNeil Forbes, Shi Jin, Rodrigo Navarro Perez, and Nicolas Schunck. Minimal nuclear energy density functional. *Physical Review C*, 97(4), April 2018.

[9] Ermal Rrapaj, Alessandro Roggero, and Jeremy W. Holt. Microscopically constrained mean-field models from chiral nuclear thermodynamics. *Physical Review C*, 93(6), June 2016.

[10] M. Dutra, O. Lourenço, J. S. Sá Martins, A. Delfino, J. R. Stone, and P. D. Stevenson. Skyrme interaction and nuclear matter constraints. *Physical Review C*, 85(3), March 2012.

[11] Charles Kittel. *Introduction to Solid State Physics*. Wiley, United States, 2004.

[12] Gaetano Senatore, Saverio Moroni, and David M. Ceperley. Static response of homogeneous quantum fluids by diffusion monte carlo. In *Quantum Monte Carlo Methods in Physics and Chemistry*, pages 183–212. Springer, Netherlands, 1999.

[13] A. Pastore, D. Davesne, and J. Navarro. Linear response of homogeneous nuclear matter with energy density functionals. *Physics Reports*, 563:1–67, March 2015.

[14] D. Davesne, M. Martini, K. Bennaceur, and J. Meyer. Nuclear response for the skyrme effective interaction with zero-range tensor terms. *Physical Review C*, 80(2), August 2009.

[15] E. Perlińska, S. G. Rohoziński, J. Dobaczewski, and W. Nazarewicz. Local density approximation for proton-neutron pairing correlations: Formalism. *Physical Review C*, 69(1), January 2004.

[16] C. García-Recio, J. Navarro, Van Giai Nguyen, and L.L. Salcedo. Response functions for infinite fermion systems with velocity dependent interactions. *Annals of Physics*, 214(2):293–340, March 1992.

[17] T.H.R. Skyrme. The effective nuclear potential. *Nuclear Physics*, 9(4):615–634, January 1958.

[18] E. Chabanat, P. Bonche, P. Haensel, J. Meyer, and R. Schaeffer. A Skyrme parametrization from subnuclear to neutron star densities. *Nuclear Physics A*, 627(4):710–746, December 1997.

[19] D. Vautherin and D.M. Brink. Hartree-Fock Calculations with Skyrme's Interaction. I. Spherical Nuclei. *Phys. Rev. C*, **5**:626–647, March 1972.

[20] E. Chabanat, P. Bonche, P. Haensel, J. Meyer, and R. Schaeffer. A Skyrme parametrization from subnuclear to neutron star densities part II. Nuclei far from stabilities. *Nuclear Physics A*, 635(1-2):231–256, May 1998.

[21] Roberto Coisson, Graziano Vernizzi, and Xiaoke Yang. Mathieu functions and numerical solutions of the Mathieu equation. In *2009 IEEE International Workshop on Open-source Software for Scientific Computation (OSSC)*. IEEE, September 2009.

[22] *NIST Digital Library of Mathematical Functions*. http://dlmf.nist.gov/, Release 1.0.24 of 2019-09-15. F. W. J. Olver, A. B. Olde Daalhuis, D. W. Lozier, B. I. Schneider, R. F. Boisvert, C. W. Clark, B. R. Miller and B. V. Saunders, eds.

[23] Nguyen Van Giai M. Beiner, H. Flocard and P. Quentin. Nuclear ground-state properties and self-consistent calculations with the Skyrme interaction (I). Spherical description. *Nucl. Phys. A*, **238**:29–69, October 1974.

[24] J.D. Hoffman. *Numerical Methods for Engineers and Scientists: Second Edition Revised and Expanded*. Mcgraw-Hill, New York, 2001.

[25] G. Wanner E. Hairer and S.P. Nørsett. *Solving Ordinary Differential Equations I: Nonstiff Problems*, edited by R. Bank, R.L. Graham, J. Stoer, R. Varga, H. Yserentant. Springer, Berlin, 2008.

[26] Eric W. Weisstein. Second-Order Ordinary Differential Equation. From MathWorld–A Wolfram Web Resource. `http://mathworld.wolfram.com/Second-OrderOrdinaryDifferentialEquation.html`, Last accessed on 13-12-19.

[27] V.G. Nguyen D. Garcia-Recio, J. Navarro and L.L. Salcedo. Response functions for infinite fermion systems with velocity dependent interactions. *Annals of Physics*, **214**:293–340, August 1992.